Impact of Mineralogy and Diagenesis on Reservoir Quality of the Lower Cretaceous Upper Mannville Formation (Alberta, Canada)

R. Deschamps[1]*, E. Kohler[1], M. Gasparrini[1], O. Durand[2], T. Euzen[3] and F. Nader[1]

1 IFP Energies nouvelles, 1-4 avenue de Bois-Préau, 92852 Rueil-Malmaison - France
2 Institut Polytechnique LaSalle Beauvais, 19 rue Pierre Waguet, BP 30313, 60026 Beauvais Cedex - France
3 IFP Technologies (Canada) Inc. 810, 744 - 4th Avenue S.W. Calgary, Alberta, T2P 3T4 - Canada
e-mail: remy.deschamps@ifpen.fr - eric.kohler@ifpen.fr - marta.gasparrini@ifpen.fr - ophelie.durand@etu.lasalle-beauvais.fr
tristan.euzen@ifp-canada.com - fadi-henri.nader@ifpen.fr

* Corresponding author

Résumé — **Impact de la minéralogie et de la diagenèse sur la qualité des réservoirs de la Formation Mannville Supérieur, Crétacé Inférieur (Alberta, Canada)** — La Formation Mannville Supérieur du Crétacé Inférieur d'Ouest-Central Alberta a été intensivement forée les précédentes décennies par des puits visant des réservoirs plus profonds. Cependant, les données de production dans ce secteur suggèrent que des volumes significatifs de gaz soient présents dans les réservoirs tant conventionnels que non conventionnels ("*tight reservoirs*") de cette formation.

Les réservoirs de la Formation Mannville Supérieur d'Ouest-Central Alberta sont constitués de grès fluviatiles remplissant des vallées incisées. Ces grès présentent une minéralogie complexe, avec des quantités variables de quartz, de feldspaths, de minéraux argileux et des fragments de roche. Ils ont été soumis à une histoire diagénétique complexe et la paragenèse qui en résulte a eu un impact sur leurs propriétés réservoirs. Par conséquent, les hétérogénéités dans les propriétés réservoirs induisent des risques significatifs en termes d'exploration et de production de ces réservoirs.

Nous présentons dans cet article les résultats de l'étude diagénétique, effectuée dans un cadre stratigraphique bien contraint, visant à comprendre l'impact de la minéralogie et de la diagenèse sur l'évolution de la qualité des réservoirs. Soixante et onze échantillons prélevés sur huit puits ont permis de réaliser une analyse pétrographique et proposer une séquence paragénétique. Quatre événements diagénétiques principaux ont été identifiés et sont liés à l'enfouissement du bassin :

– coating d'argile autour des grains;
– compaction/dissolution de grains matriciels;
– dissolution partielle des grains de quartz et de feldspaths, qui ont initiés la transformation smectite-illite et kaolinisation;
– cimentation carbonatée dans l'espace poreux restant.

Les transformations de minéraux argileux et la cimentation carbonatée sont les facteurs principaux qui ont affecté la porosité et la perméabilité de ces grès. La transformation Smectite-Illite a été amorcée après que le potassium issu de la dissolution des feldspaths ait été libéré dans le fluide de formation. Cette transformation augmente proportionnellement avec l'enfouissement et la température. Une intense cimentation carbonatée est survenue pendant la phase de soulèvement du bassin, colmatant de façon très significative l'espace poreux là où la teneur en argile était réduite.

Des analyses au Microscope Électronique à Balayage et des analyses de DRX ont permis de caractériser et d'évaluer quantitativement les différentes phases diagénétiques responsables de l'évolution de l'espace poreux.

La caractérisation de la minéralogie et de l'évolution des propriétés pétrophysiques des réservoirs apportent des clés utiles pour localiser les différentes phases diagénétiques temporellement et spatialement, afin de prédire la distribution de propriétés pétrophysiques.

Abstract – Impact of Mineralogy and Diagenesis on Reservoir Quality of the Lower Cretaceous Upper Mannville Formation (Alberta, Canada) – The Lower Cretaceous Upper Mannville Formation in West-Central Alberta has been intensively penetrated by wells targeting deeper reservoirs during the last decades. Production and well log data in this area suggest that significant volumes of gas are still present in both conventional and tight reservoirs of this formation.

The Upper Mannville reservoirs in West-Central Alberta consist of fluvial sandstones filling incised valleys. The valley infills are made up of arkosic sandstones with a complex mineralogy. The matrix of these sandstones is made up of various amounts of quartz, feldspars, clay minerals and rock fragments. They were subjected to a complex diagenetic history and the resulting paragenesis influenced the present reservoir properties. Consequently, heterogeneities in the petrophysical properties result in significant exploration risks and production issues.

We present in this paper results of a diagenetic study, performed within a well constrained stratigraphic framework, that aims at understanding the impact of mineralogy and diagenesis on reservoir quality evolution. Seventy one core samples from eight wells were collected to perform a petrographic analysis, and to propose a paragenetic sequence. Four main diagenetic events were identified that occurred during burial:

– clay coating around the grains;
– compaction/dissolution of matrix grains;
– quartz and feldspars dissolution that initiated smectite-illite transformation and kaolinisation;
– carbonate cementation in the remaining pore space.

Clay minerals content and carbonate cementation are the main factors that altered the reservoir quality of these sandstones. The Smectite-Illite transformation was initiated after potassium was released in the formation fluids due to K-feldspars dissolution. This transformation proportionally increased with temperature during burial. Carbonate cementation occured during the uplift phase of the basin, intensively plugging the pore space where the clay content is reduced.

Additional SEM and XRD analyses allowed characterizing and quantifying more accurately the different mineralogical phases occluding the porous network. The characterization of both mineralogy and petrophysical properties gives useful keys to locate the diagenetic phases laterally and vertically, and to predict the petrophysical properties distribution.

INTRODUCTION

The Lower Cretaceous Mannville group (MNVL) contains one of the main oil and gas bearing reservoirs of the Western Canadian Sedimentary Basin (WCSB). Although the Lower Mannville has been extensively drilled over the past decades, the Upper Mannville interval remains relatively immature in regard to exploration for gas charged reservoirs. This is particularly true in Central Alberta, where the Upper Mannville reservoirs are formed as incised valley fill, and are therefore mostly discontinuous sand bodies. Furthermore, the arkosic nature of these sandstones and their diagenetic evolution strongly impact the reservoir, making it more difficult to recognize potential plays.

The key to successful exploration in such a difficult play lies in the effective integration of geological, reservoir engineering and geophysics data. Regional correlations were performed in order to establish a reference stratigraphic framework of the Upper Mannville, which is currently designated as undivided in Central Alberta (Cant, 1996). This sequential organization was then used to correlate and map incised valley trends over smaller areas (Deschamps *et al.*, 2008).

In this paper, we present an integrated methodology leading to the mineralogical characterization and diagenetic phases quantification of the Upper Mannville incised valley fill in Central Alberta, whithin a well constrained stratigraphic framework

Diagenetic heterogeneities strongly influence reservoir performance and fluid flow. Predicting reservoir heterogeneities in such a mineralogically complex and diagenetically altered succession remains a crucial point for less risky exploration and production (Bloch *et al.*, 1994; De Ros, 1996; Morad *et al.*, 2010; Pittman *et al.*, 1989). To assess the importance of the diagenetic transformations that occurred in the sandstones during the basin history, diagenetic events

have been characterized thanks to the petrographical description of core samples taken on several key wells cored in the incised valleys fill.

Quantifying diagenetic phases is one of the challenges to predict the diagenetic heterogeneity distribution at both basin and reservoir scales. A new approach for diagenetic phase quantification is presented in this paper that aims at assessing the reservoir quality evolution through the different diagenetic events described in the paragenesis, in terms of type and percentage of porosity loss or enhancement. This method is developed by using SEM and EDS analyses, that provide quantitative mineral maps of the studied samples, allowing reconstructing the porosity evolution linked with diagenetic phases, excluding the compaction effect, which is difficult to assess by using these methods.

1 GEOLOGICAL SETTING

1.1 Western Canada Sedimentary Basin (WCSB)

The Western Canada Sedimentary Basin (WCSB) is a northeast-southwest trending clastic wedge encompassing an area of approximately two million km² (Osadetz, 1989). This basin extends eastward from the Foreland Belt of the Canadian Cordillera towards the Canadian Shield *(Fig. 1)* (Strobl, 1988), and is well known for its vast amount of conventional and unconventional hydrocarbon resources, particularly in Alberta, Saskatchewan and Northeastern British Columbia. The wedge reaches a maximum thickness of approximately 6 000 m in the axis of the Alberta Syncline east of the foothills front and thins out to zero in the northeast towards the Canadian Shield (Wright, 1984).

The WCSB can be sub-divided into two major groups that reflect the sedimentation linked to two unrelated tectonic settings *(Fig. 2)*:

– Paleozoic-Jurassic succession that is dominated by carbonate sedimentation, and deposited atop the stable craton next to North America's earlier passive margin;
– Mid-Jurassic-Paleocene foreland basin succession overlying the previous carbonate succession and mainly consisting of clastic deposits formed during the uplift of the Canadian Cordillera.

Following these two successions and the Laramide Orogeny culmination during the Paleocene, net erosion and sediment by-pass have prevailed thereafter.

Two distinct subsidence episodes from Late Jurassic (Oxfordian) to Early Cretaceous and from the Aptian to Eocene were linked to the orogenic activities, and thus occurred in the Foreland Basin. A major unconformity ranging from 10 to 20 My developed between these two stages (Cant, 1996), being related to an uplift and tilting phase linked with the Rockies belt orogeny. During Aptian time, the
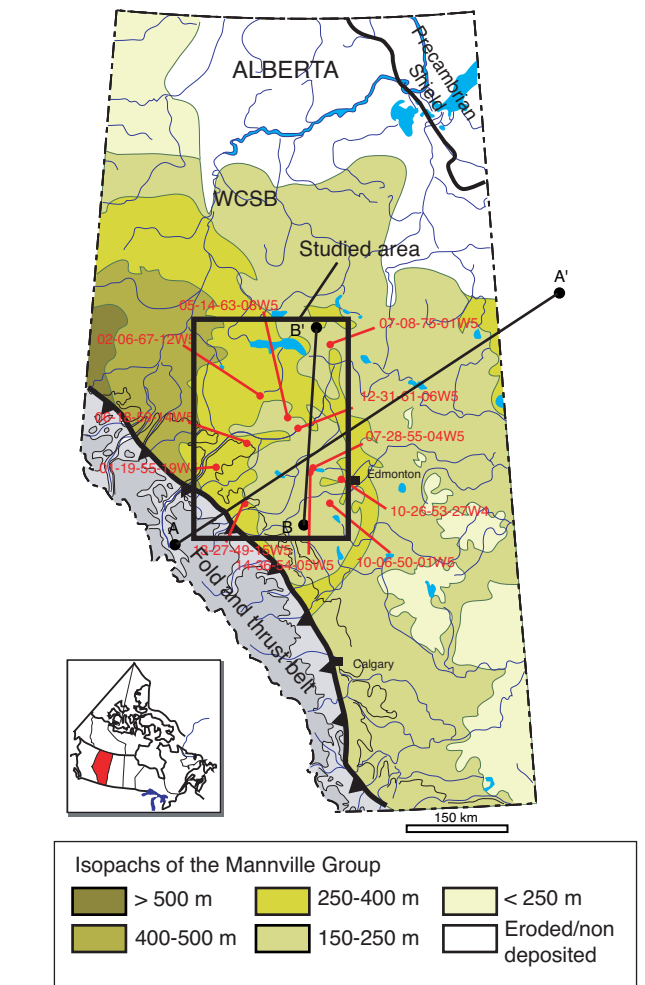

Figure 1

Location map of the studied area, with sampled wells location, isopachs of the Mannville Group, and position of the transects A-A' and B-B', respectively presented in Figures 2 and 5.

sea invaded from the north and eventually covered the topography. The Mannville Group was deposited above the unconformity separating these two stratigraphic assemblages, overlying tilted and truncated strata ranging from the Paleozoic to the Mesozoic Eras (Jackson, 1984; Cant, 1996). Hence, the topographic relief below the unconformity was controlled by tectonic factors and a differential erosion of underlying units (Hayes *et al.*, 1994). The development of major valley systems was dominant prior to the deposition of younger overlying sediments such as the Mannville Group (Poulton *et al.*, 1994).

The maturation and temperature history from Triassic to present day was calculated by using vitrinite reflectance on the well already used by Higley *et al.* (2009) for burial
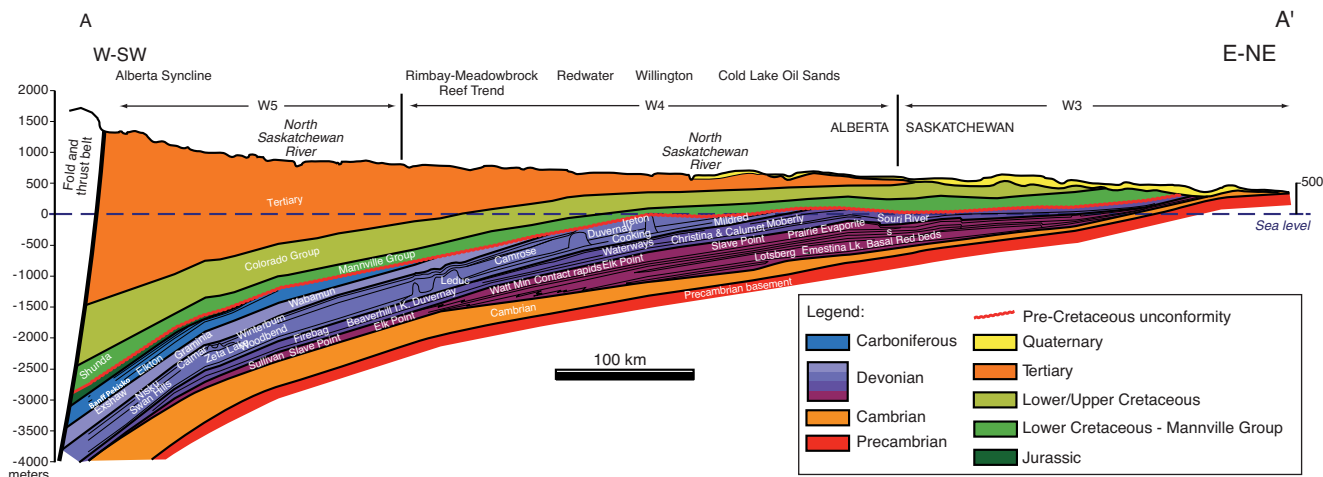
Figure 2

West-South West – East-North East geological section across the Western Canada Sedimentary Basin, east of the Cordilleran Fold and Thrust Belt (modified from Wright, 1984). Vertical exageration is approximately 40 times.

history reconstruction, assuming an average thermal gradient of 25°C per kilometer. In the studied area, the average sediment thickness eroded since about 58 My reaches 1580 m, according to the modelling performed by Higley *et al.* (2009).

1.2 Mannville Group Overview

The Mannville Group is a clastic wedge deposited during Barremian-Aptian to Early Albian times (± 120 to 104 My?) in the Western Canada Foreland Basin *(Fig. 3)*. This group forms part of the Lower Zuni Sequence deposited in the WCSB (Cant, 1989). It can reach up to 700 m in thickness towards the foothills near the western margin of the basin, but ranges from about 115 to 265 m in the study area. Unlike for the other parts of the clastic wedge of the WCSB, the sedimentary supply during the Mannville stage came from the south and was parallel to the basin axis (*i.e.* longitudinal), as opposed to the more usual orthogonal pattern of deposition relative to the hingeline (Cant, 1996).

The Lower Mannville consists of non-marine strata resting directly on top of the basal unconformity (Cant, 1996) *(Fig. 3)*. This transgressive phase leads to the deposition of fluvial sediments along the topographic lows that cut through less competent strata of the underlying unconformity. The sediments pass upward to estuarine/tidal and shoreface facies (marginal marine deposits) and are sealed by offshore marine shales corresponding to the MFS of the same order sequence. The transgressive cycles developed from the north-northwest, and the deposition of Lower Mannville sediments was strongly influenced by the topography of the sub-Cretaceous unconformity.
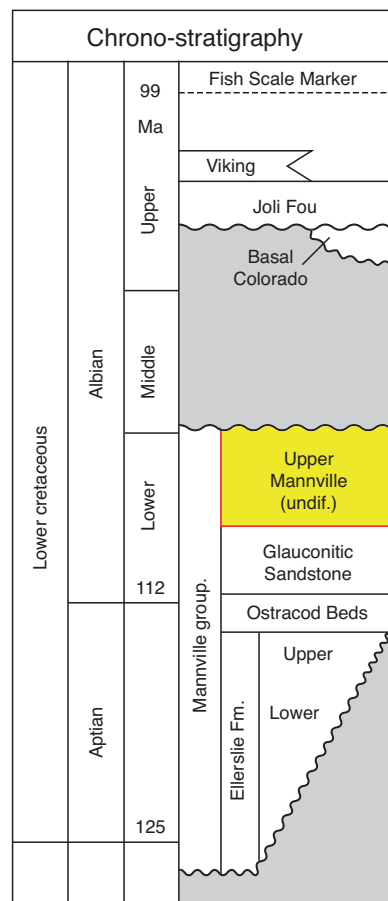

Figure 3

General stratigraphy of the Lower Cretaceous in Central Alberta.

The Upper Mannville consists of shallow marine sediments that progressively pass to coastal plain and fluvio-continental facies. It contains a series of successive progradations across the entire basin in a north-northwest direction, as shown by Jackson (1984). Moreover, the regressive phase of the Upper Mannville included shorelines that prograded for more than 300 miles (480 km) northward towards the offshore setting (Jackson, 1984).

The overall depositional sequence of the Mannville Group can be subdivided into three main stages:

– fluvial networks oriented towards the northwest and draining through structural lows controlled by the pre-Mannville paleo-topography and subsequent incisions (Lower Mannville);

– marine transgression followed by progradation in wave-dominated settings (informal "Middle" Mannville);

– continuous regressive sedimentation in continental to shallow marine environment dominated by northward fluvial systems (Upper Mannville) (Cant, 1996).

The sediments were deposited in the fluvial incised valleys and floodplains. They were derived from a positive topography in the orogenic area located in south-central British Columbia, *i.e.* in the rising Rocky Mountains to the west of the Central Alberta Plains. The Rocky Mountains were composed of accreted terranes including plutonic belts, volcanic as well as metamorphic rocks (Wyld *et al.*, 2006).

1.3 Burial History and Petroleum Systems

The Mannville Group presents a prolific and extensive hydrocarbon potential varying from coal, conventional oil, unconventional oil (a.k.a. heavy oil), tar sands, as well as natural gas. The coal measures were deposited in coastal plain environments and are mainly preserved in the present-day foothills. The oil and gas are generally trapped within sandstone reservoirs of fluvial and incised valley-fill features in the southern and eastern regions, while in the northern and central regions they are trapped in more widely distributed shoreline sandstone complexes marking lateral facies change due to shoreface deposits migration (pinchouts). As a result, the majority of the traps occurring within the Mannville Group relate to stratigraphic traps (Putnam, 1982; Hayes *et al.*, 1994).

The main potential source rocks in this area relate to the Devonian Duverney Formation, the Devonian-Mississipian Exshaw Fm., the Triassic Doig Fm., the Jurassic Fernie Group, and the Lower Cretaceous Mannville coals and Ostracod Zone (Creaney *et al.*, 1994; Riediger *et al.*, 1997; Higley *et al.*, 2009). Higley *et al.* (2009) performed a 4D petroleum modeling in the studied area, to assess the source and timing of oil generation for the Lower Cretaceous Mannville Group in the Northern Alberta (oil sands). As a result of the model, burial history reconstruction was

established. This model also evidenced that maturation and HC migration from the source rocks started prior to the onset of the general uplift and erosion, *i.e.* between the Late Cretaceous (~75 Ma) and the Early Paleogene (~58 Ma) (Higley *et al.*, 2009). However, due to the lack of key traps surrounding the source rocks, most of the hydrocarbon migrated updip in a general eastward direction towards the surface (Riediger *et al.*, 1999; Schneider, 2003; Faure *et al.*, 2004).

The depositional and erosional trends were based on a 1D extraction of a 4D model in the studied area. The construction of burial curves shows that three distinct phases of vertical motion occurred after the Mannville deposition (Faure *et al.*, 2004; Highley *et al.*, 2009):

– a gentle subsidence phase between 115 Ma and 80 Ma;

– a rapide subsidence phase between 80 Ma and 58 Ma, due to the tectonic loading linked to the Late Cretaceous to Paleocene thrusting in the Southern Canadian Rocky Mountains foothills and eastern front ranges;

– uplift and erosion during the Early Tertiary Laramide orogeny (Higley *et al.*, 2009).

2 UPPER MANNVILLE SEDIMENTARY SYSTEM

2.1 Regional Stratigraphic Correlations

High resolution stratigraphic correlation was first performed at a regional scale in order to define the stratigraphic archi-tecture of the Upper Mannville in the studied area (Deschamps *et al.*, 2008). This correlation was based on the analysis of log stacking patterns, calibrated on core descrip-tions, and on regional facies transition from continental to marine environment *(Fig. 4)*.

Higher order correlatable cycles identified within the Upper Mannville outline a network of incised valleys formed following a relative sea level fall of variable amplitude. Furthermore, during the subsequent sea level rise, these incised valleys were usually filled up with estuarine to fluvial sediments.

Nine sequences have been recognized in the Upper Mannville at regional scale. Some of them are however merging eastward, probably because of a decreasing subsidence rate when moving away from the Lamarian thrust belt. In the studied area, seven correlatable sequences have been identified. The sequences 1 and 2 correspond to marine deposits. The sequence 3 is transitional between marine and continental environment, whereas the sequences 4 to 7 were deposited in a continental setting. The incised valleys of these 4 uppermost sequences are filled with fluvial sediments, which correspond to the main exploration target of the Upper Mannville interval in this area.
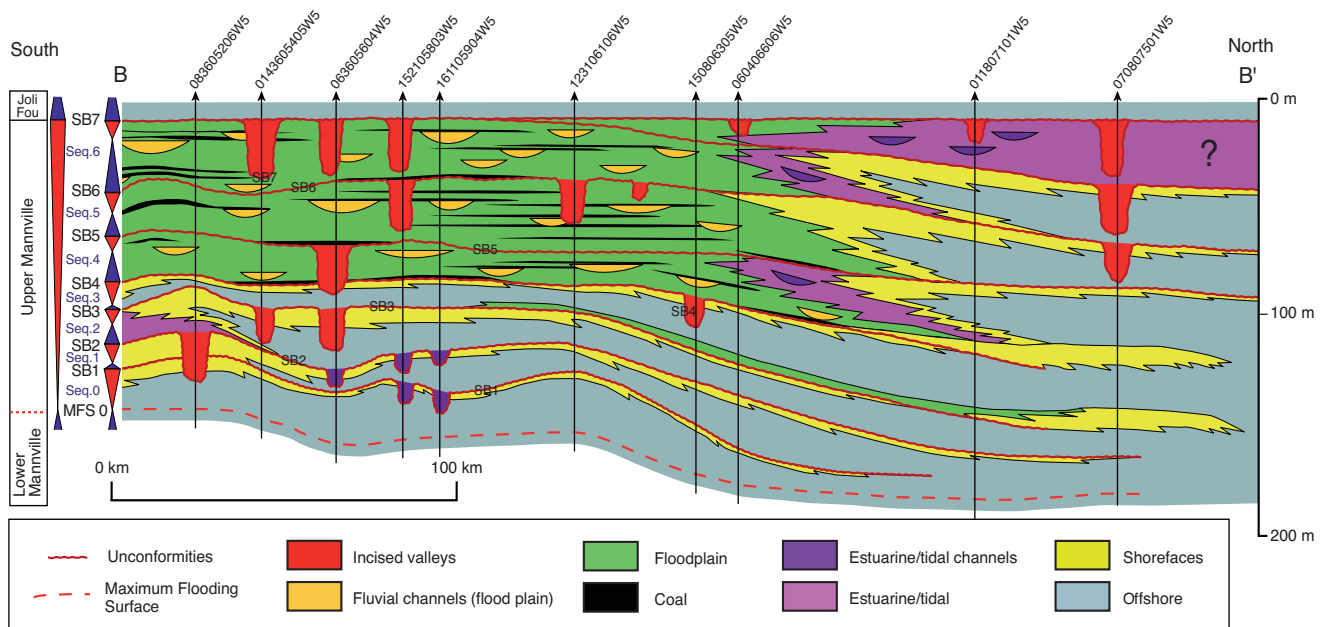
Figure 4

North-South stratigraphic correlation transect and facies evolution of the Upper Mannville Formation in West-Central Alberta.

2.2 Incised Valley Fill

The sandstone lithology in the Mannville Group shows an abrupt contrast from a quartz and chert-rich succession in the Lower Mannville to a more volcanic and feldspathic-rich composition in the Upper Mannville (Hayes *et al.*, 1994). The Mannville Group as a whole is unconformably overlain by clastic rocks from the Colorado Group (Karavas *et al.*, 1998).

In the studied area, the incised valley fill of the uppermost Upper Mannville sequences is made up of stacked braided fluvial channels, whose thicknesses usually reach 25 to 30 m at the maximum of incision *(Fig. 5)*. Braided fluvial amalgamated channels are generally seen at the base of the valley fill, with a sharp contact with the underlying but genetically unrelated sediments. Mud and coal clasts are locally abundant, forming a lag at the base of the valley fill, which is marked by a deflection of the Neutron-porosity and sonic logs. Braided amalgamated fluvial channels are deposited in a high energy system, at the beginning of the base level rise. The continuous rise of the base level induced the flattening of the depositional profile within the valley, accompanied by a decrease of the transport energy. Above the basal fluvial sandstones, meandering/anastomosed isolated channels and flooplain to coastal plain deposits testify of the backstepping evolution of the fluvial system during a transgression.

From cores observations, the Upper Mannville reservoir quality is considered to be poor to average, depending on the heterogeneous distribution of preserved pores and the diagenetic effects upon them. The Upper Mannville fluvial reservoirs are considered to be unconventional "tight reservoirs" in the studied area (see porosity estimates in *Tab. 1*). The braided fluvial valley fill sandstones are mostly composed of arkose and to a lesser amount of litharenites, whose porosity is partly controled by diagenetic processes (Euzen *et al.*, 2011). The meso-scale porosity consists of remnant intergranular pores and secondary pores associated with grain dissolution. The pore space is locally completely cemented by calcite.

3 PETROGRAPHIC AND DIAGENETIC STUDY

3.1 Database and Methods

Approximately 100 samples were collected from the cores of 11 wells in the studied area *(Fig. 1)*. These samples were taken from the incised valley fill from sequences 4 to 7 *(Fig. 4, 5)*, that correspond to braided fluvial channel fill.

Seventy one thin-sections were prepared for petrographic observations. All the thin-sections were stained with alizarin red-S and potassium ferricyanide to differentiate carbonate
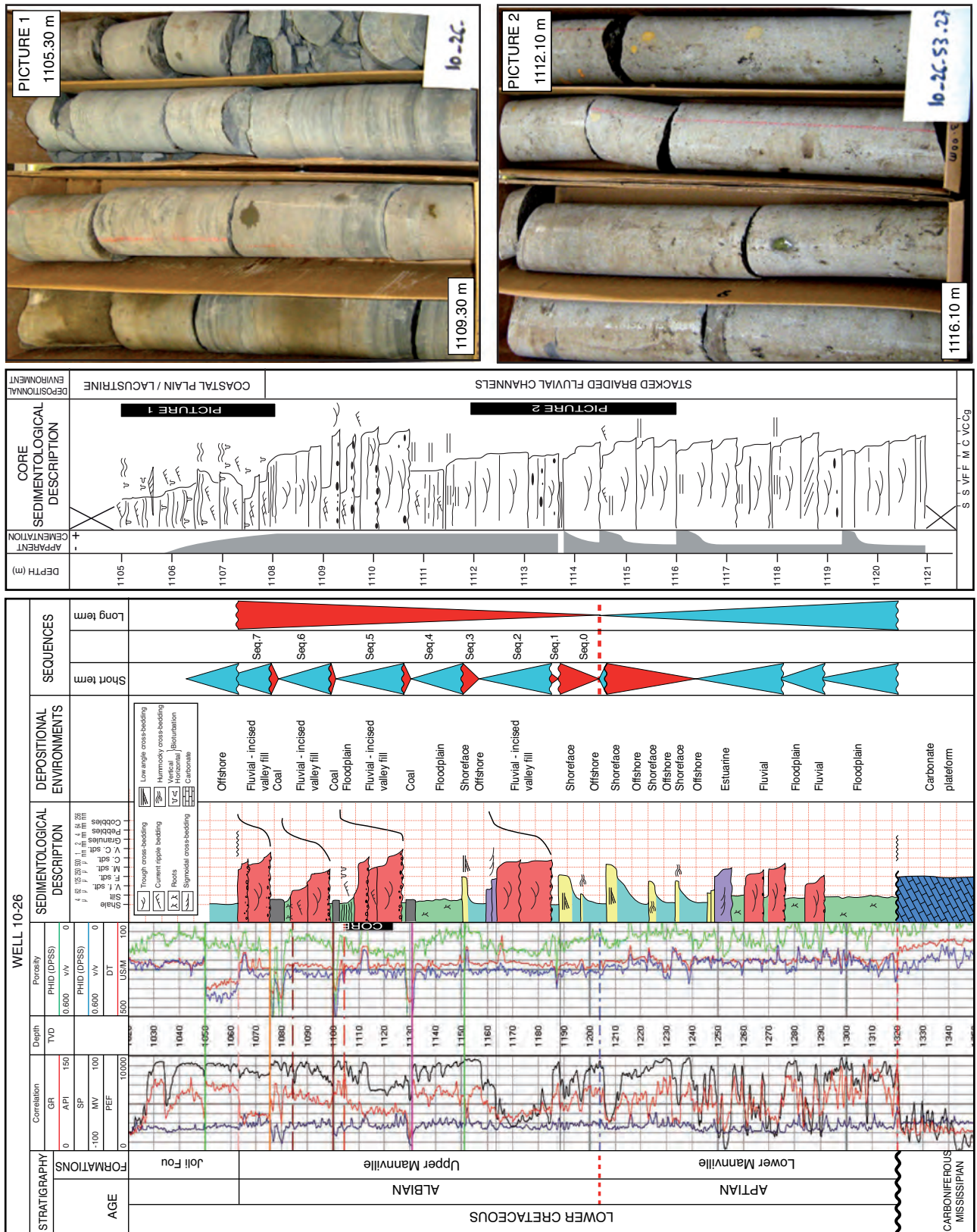
Figure 5

Reference well log sedimentological interpretation of the Upper Mannville interval, with sedimentological description, core description, and illustrations of the main facies on core.

minerals and asses the distribution of ferrous iron. Petrographic observations included conventional, UV-light and cathodoluminescence (CL) microscopy. The latter was performed with a Technosyn Cold CL Model 8200 Mark II (OPEA, France). Operation conditions were 16-20 kV gun potential, 420-600 μA beam current, 0.05 Torr vacuum and 5 mm beam width.

Among these samples, twenty two were chosen for petrographic observations, representative of the mineralogical variability of the sample dataset, and therefore, were also prepared for bulk XRD analysis. The samples were analyzed with an analytical X'pert PRO PW 3040/60. The diffractometer operated at 50 kV, 30 mA and scanned samples in the 2θ range from 2 to 80° with a step size of 0.033° (2θ)/s. The counting time was 200 minutes for each sample.

Fifteen bulk powders from the most carbonate-rich samples belonging to 7 different wells were obtained from rock slabs by means of a dental drill. Carbonate phases for these samples account to 15 to 35% in volume. Analyses to determine the O and C isotope ratios were performed at the Friedrich-Alexander-Universität of Erlanden-Nürnberg (Germany). Carbonate powders were reacted with 100% phosphoric acid at 75°C using a Kiel III carbonate preparation line connected online to a ThermoFinnigan 252 masspectrometer. All values are reported in permil relative to V-PDB by assigning a $\delta^{13}C$ value of +1.95‰ and a $\delta^{18}O$ value of -2.20‰ to NBS19. Reproducibility was checked by replicate analyses of laboratory standards and is better than ±0.01‰ and ±0.08‰ for $\delta^{13}C$ and $\delta^{18}O$, respectively. In this study, the $\delta^{18}O$ notation without any further specification will be referred to the V-PDB standard. The oxygen composition of present and past fluids will be expressed relative to the SMOW international standard and referred as $\delta^{18}O_{SMOW}$.

EDS and SEM analysis were performed on 5 samples for compositional analysis (punctual analysis for chemical compostion and mineral mapping). The quantification process was made using the SEM for compositional analysis (ponctual analysis for chemical composition, and mineral mapping). Material balance from diagenetic water-rock interactions based on 2D chemical mapping can thus be estimated.

The SEM used is a Zeiss EVO SEM, Oxford ESS. The operating conditions for punctual analysis were HT = 15 kV, I_{probe} = 700 pA, and the dead time less than 35%. For the spectral imaging, the time cunting was 1 000 microseconds, and the acquisition time was 1 h 30 min for 86 × 128 pixels. The analysis were performed in order to map mineralogical assemblages and to determine porosity changes associated to mineralogical transformations through the diagenetic events. X-ray intensity maps of all elements were transformed to oxide wt.% with Oxford software constrained by EDS standardisation. Statistical cluster analysis was used to identify the different phases occurring in the samples. Based

on the work of De Andrade *et al.* (2006), matlab sofware was developed to compute the data coming from SEM analysis.

Image analysis has been performed on 23 representative samples. The aim is to estimate the amount of the main mineral constituents (*i.e.* quartz, feldspars, clays, carbonates) and porosity, by extracting with threshold methods the different colours on scanned thin-sections. The software used is "JMicroVision", a freeware designed to describe, measure, quantify and classify components of all kinds of images and especially developed to analyze high definition images of rock thin-sections (http://www.jmicrovision.com/index.htm). These data, compiled in Table 1 must be used with care, as they only represent a rough estimation of the components on 2D images.

3.2 General Petrographic Description

The sandstone composition of the Upper Mannville incised valley fill ranges from arkose to litharenite but can be mostly referred to arkose, according to Folk's classification (Folk, 1970; *Fig. 6*), with variable proportions of detrital clays. Variable amounts of clay minerals and carbonates are also present in the samples as a result of diagenesis. Most samples correspond to poorly sorted angular to sub-angular medium grained sandstones. Coarse grained sandstones to conglomer-ates can be observed and correspond to channel basal lags at the base of the incised valley fill, or to internal fluvial erosional surfaces. Conglomerates are also observed at the Top Mannville Formation, probably corresponding to the Basal Colorado.
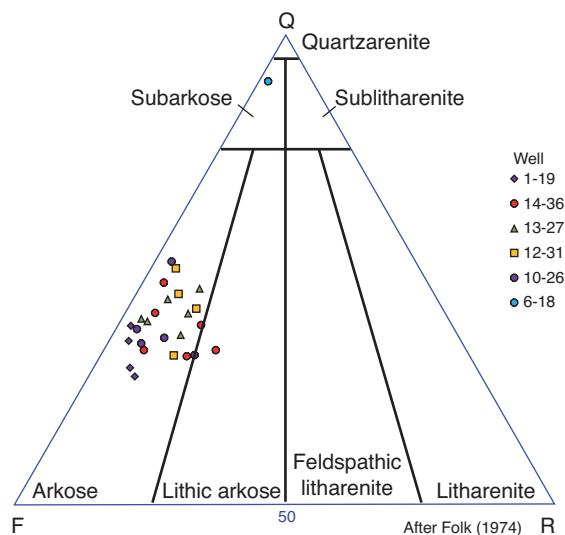

Figure 6

Position of the studied samples in Folk's sandstone classification.

TABLE 1

Relative proportions of the various mineralogical constituents of the Upper Mannville sandstonee, with location of the sample in the sequential framework, position in present day depth, estimated maximum burial depth and associated estimated temperature reached by the samples

SAMPLES	Present day depth (m)	Estimated max. burial depth (m)	Estimated max. T°	Depositiomnal environment/Sequence	Quartz (%total volume)	Feldspars (%total volume)	Indiff. clays (%total volume)	Interstrat. clays (%total volume)	Chlorite (%total volume)	Biotite (%total volume)	Muscovite (% total volume)	Organics (%total volume)	Siderite (%total volume)	Lithic fragments (%total volume)	Carbonate cement (%total volume)	Undifferenciated (%total volume)	Porosity (%total volume)
1-19_4	2 552.2	4 052.2	101	Incised valley/7	12	13.9	1	1.7	1.6	0.3	1	0	34.3	3	31.2	0	0
1-19_5	2 550.3	4 050.3	101	Incised valley/7	28.3	23.8	8.7	6.2	3.2	1.1	4.4	0	2.7	6.7	14.9	0	0
1-19_6	2 548.8	4 048.8	101	Incised valley/7	31.7	25	12.7	10	0	0	0.75	0	1	5.75	2	4.3	6.8
14-36_2	1 277.1	2 777.1	70	Incised valley/7	27	30	14.6	7	4.4	0.5	3	1	1.5	3	0.5	0	7.5
14-36_2bis	1 274	2 774	70	Incised valley/7	9.7	13.7	0.7	0	0	0	0	3.8	47.7	6	15.7	0	2.7
14-36_3	1 273.1	2 773.1	70	Incised valley/7	17.7	15	4.2	2.8	2	1	2.8	2	15	3.6	26.6	3	4.3
14-36_6	1 268.2	2 768.2	70	Incised valley/7	28	24.7	6.7	5.1	4.7	1.2	1.7	2	17	0	8.9	0	0
14-36_7	1 266.8	2 766.8	70	Incised valley/7	30.3	29	6.2	5.6	3.2	0.2	0.3	11.9	7.2	0	0	2.4	3.7
14-36_8	1 266.2	2 766.2	70	Incised valley/7	22	31.2	8.3	13	2.3	0	0.3	0.2	4	10	0	0	8.7
14-36_10	1 264.6	2 764.6	70	Incised valley/7	26	28	5	5	3.2	0.4	0.5	1.4	2	0	28.5	0	0
14-36_16	1 252.5	2 752.5	70	Incised valley/7	23.7	32.1	10.6	7.6	0.4	0.4	0.2	0	12	2.1	8.1	0	2.8
14-36_19	1 251	2 751	70	Incised valley/7	34.9	34.4	12.8	6.7	5	0.3	2.2	1.6	2.1	0	0	0	0
13-27_1	2 583.6	4 083.6	102	Incised valley/7	64.3	16.6	8.4	4.9	0.2	0.7	0.3	2.5	0.5	1.4	0.2	0	0
13-27_2	2 581.5	4 081.5	102	Incised valley/7	34.9	25.5	8.4	5	9.6	0.2	4.5	0.7	7.2	1.2	2.8	0	0
13-27_5	2 578	4 078	102	Incised valley/7	26.2	24.4	12.5	7.4	8.9	0.2	0	0.1	7.4	1.3	2.8	0	8.8
13-27_12	2 566.5	4 066.5	102	Incised valley/7	30.2	26.7	5.4	7.2	8.6	0	0	0	2.2	3.2	14.3	0.4	1.8
12-31_2	969.6	2 469.6	62	Incised valley/6	29.6	23.3	18.9	8.2	4.9	0.1	1.6	0	7.8	1.4	0	0	4.2
10-26_1	1 120.8	2 620.8	65	Incised valley/5	28.8	30.2	4.6	5.4	4.3	0	1.1	0	2.3	1.5	20.6	0	1.2
10-26_2	1 119.2	2 619.2	65	Incised valley/5	27.3	29.3	17.2	6.9	4.3	0.7	2.3	0.2	1.8	2.6	1.4	0	6
10-26_4	1 116.2	2 616.2	65	Incised valley/5	25.9	26.2	17	6.1	3	4	1.8	0	4.7	1.4	7.8	0	2.1
10-26_5	1 114.5	2 614.5	65	Incised valley/5	26.1	25.9	22	7.1	3.2	0	1.1	0	3.4	3.2	6	2	0
6-18_6	1 755.5	3 255.5	81	Basal Colorado	77.5	5.9	2.8	3.3	0.2	0	0	4.1	0	0.2	0	0	6
7-28_5	1 255.6	2 755.6	79	Incised valley/7	19.6	23.6	5.9	3.8	0.2	2	1.2	0.4	4.5	3.2	32	1	2.6

The proportion of shaly matrix varies between 0% to more than 40% in incised valleys from older sequences (sequence 5, *Fig. 5*). This suggests a more distal position relative to the source area, and/or a different source compared to the younger sequences 6 and 7 (Euzen *et al.*, 2010). These observations are consistent with the overall prograding trend of the Upper Mannville towards the North *(Fig. 5)*. Black to reddish stratiform seams of organic matter are found in some intervals.

Detailed mineralogical observations and point counting on the most representative samples have shown the complex and variable mineralogical composition of the sandstones at the scale of both the valley fill sequence and the whole studied area. This variability is mainly controlled by the proportions of matrix clays, authigenic clays, carbonate cements and siderite. The latter is mostly present as detrital grains forming lags at the base of the channel fill, and less commonly as authigenic mineral.

3.2.1 Detrital Minerals

Quartz, feldspars, and in a lesser proportion clay minerals and rock fragments, are the main framework constituents of the Upper Mannville incised valley fill. Opaque minerals, micas (biotite and muscovite), and heavy minerals occur as accessory constituents, but have an impact on the diagenetic reactions that occurred during burial. Composition and proportions of minerals of the Upper Mannville fluvial sandstones are shown in Table 1. Quartz and feldspars are the major primary constituents of these sandstones. Mud aggregates served as framework grains as well, but their proportions are quite difficult to assess because of the compaction effect during burial, and the later diagenetic transformations. Illustrations of the main mineralogic phases are displayed in Figures 7 and 8.

The paleodrainage reconstruction made by Eisbacher *et al.* (1974) suggests that the source area for this material corresponds to the western Rocky Mountains and intrusives of the Omineca Crystaline belt. The sediments were transported northerly along the axis of the central part of the southern foreland basin towards the marine embayment northwards which occupied west-central Saskatchewan (Jackson, 1984).

Quartz grains correspond to monocristalline quartz ranging from very fine to medium grained angular to sub-angular, to rounded pebbles forming lags at the base of the fluvial channels. Some of the grains are fractured. If we exclude basal lags, quartz proportions range from 18% to 35% of the studied core samples *(Tab. 1)*. Some quartz grains are partially dissolved and replaced by carbonate cements *(Fig. 7a)*.

Feldspars are also very abundant framework grains, as their proportion exceeds 25% in most of the studied samples *(Tab. 1)*. Both plagioclases (mostly albite and to a less degree anorthites) and potassic feldspars (mostly microcline) are commonly present in the samples. Albite is the predominant type of feldspar observed. Most feldspar grains are slightly affected by alteration and dissolution. Albitization and carbonate replacement *(Fig. 7b-d)* are frequently observed, leaving irregular grain morphologies, but kaolinitization *(Fig. 7e, f)* and illitisation are the most common types of feldspars alteration. Some feldspar and quartz grains exhibit internal dissolution, constituying secondary porosity.

Rock fragments occur in a minor amount. Some metamorphic rock fragments have been documented. Micas (biotite and muscovite) abundance ranges between 1% and 5%, and heavy minerals like Rutilium and Zirconium are also commonly found, coming from unroofing of plutons in the source area westward, dated between 113 and 174 my according to Norris (1964).

Siderite generally forms under organic-rich highly reducing conditions (Curtis *et al.*, 1975). The most favorable environments for siderite formation are organic-rich reducing fresh water systems like swamps, marshes and lakes (Postma,

1982; Zodrow *et al.*, 1996). The siderite grains found in the Upper Mannville incised valley fill may come from the erosion of the coal-rich floodplain deposits constituying the background sediments deposited during the highstand periods and incised during lowstand periods. Another origin for the siderite can be inferred, as early clay clasts replacement at the base of the channel fill. In this case, siderite corresponds to an authigenic mineral.

Black to reddish stratiform organic matter seams, showing no fluorescence under UV-light (continental origin) and locally pyritised, were also observed on many samples *(Fig. 7g)*.

3.2.2 Authigenic Minerals

The diagenetic minerals of the Upper Mannville incised valley fill consist of clay minerals (chlorite, kaolins, interstratified mixed layer illite/smectite, and illite), carbonate cements (calcite, dolomite), plagioclases (albite), and pyrite. Quartz overgrowths have not been observed in the studied samples.

Clay Minerals
Authigenic clay minerals in the Upper Mannville fluvial sandstones have been determined by both microscopy and bulk XRD analysis on 27 samples. The authigenic clay minerals occur as pore lining, pore filling and detrital grains replacement types. Clay rim cement is observed on most of the studied samples forming coating around detrital grains *(Fig. 7b, h)*. Pore filling clay minerals mostly correspond to mixed layer illite/smectite and illite minerals. Clay minerals replacing detrital grains are mainly illite and kaolins:

– *Chlorite*: Chlorite is found in almost all the studied samples. The proportion of chlorite ranges between 0% and 10% *(Tab. 1)*. Chlorite occurs as detrital grains *(Fig. 8a)*, as replacement of micas *(Fig. 8b)* and as a pore filling mineral;

– *Mixed layer illite/smectite (I/S) minerals*: Mixed-layer illite/smectite have been identified with XRD analysis, and are present in variable proportions in the studied samples, ranging from 0% to 13%, with an average around 6% of the total rock volume *(Tab. 1)*.

Mixed-layer illite/smectite minerals usually appear in transmitted light as dark-brown slightly opaquous phases filling the pore space. These minerals probably originated from the transformation of clay detrital grains (smectite), and have been deformed by compaction up until occupying the whole pore space, due to the ductile behaviour of clay minerals.

These authigenic clays are the results of the smectite transformation into illite, which occurs during burial by temperature increasing with depth (Meunier, 2005; Zhang *et al.*, 2004). The proportion of illite minerals in the mixed-layer illite/smectite increases continuously with burial. The XRD analysis show several steps of smectite illitization.

R Deschamps et al. / *Impact of Mineralogy and Diagenesis on Reservoir Quality of the Lower Cretaceous Upper Mannville Formation (Alberta, Canada)*
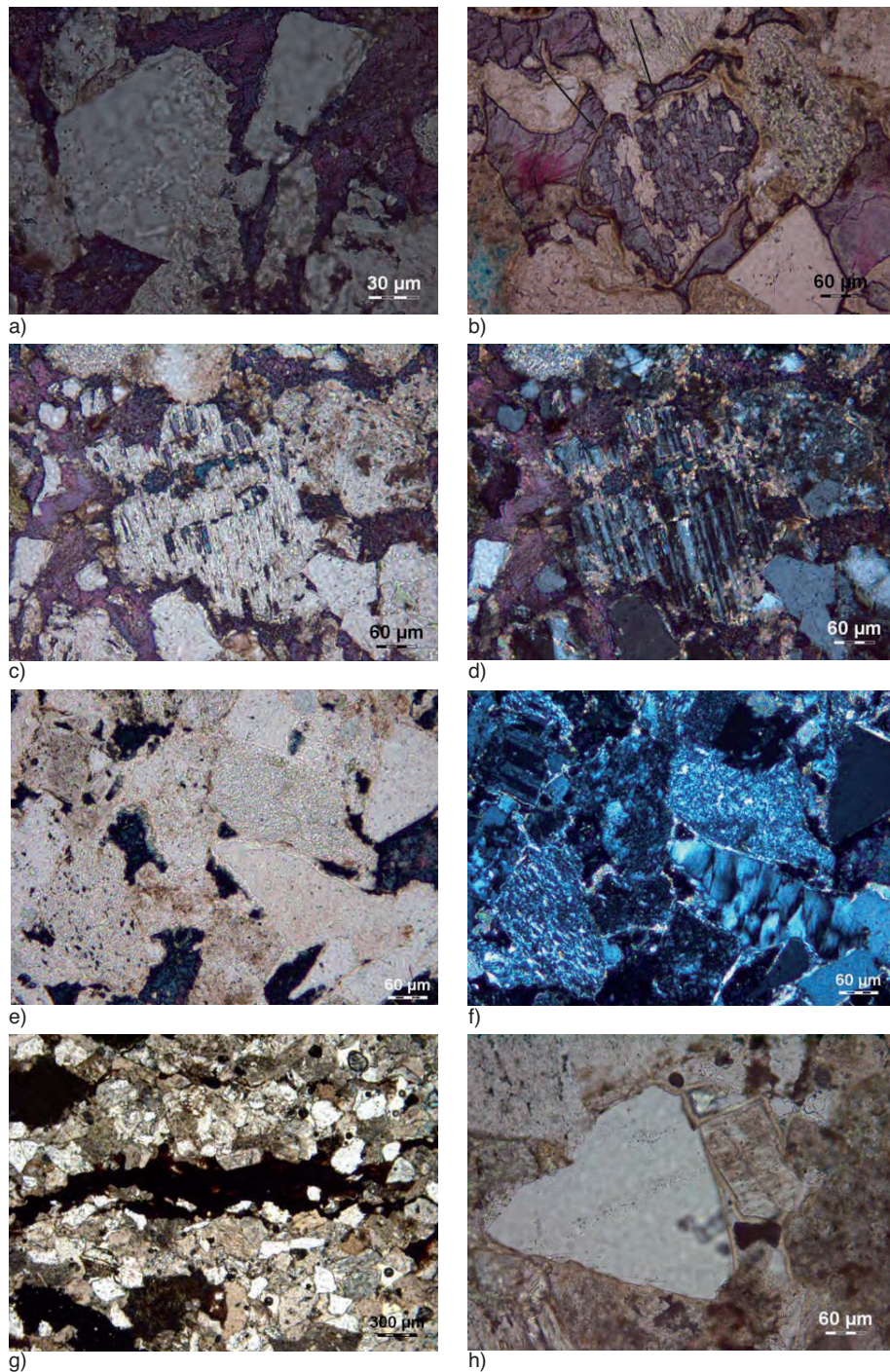
41

Figure 7

Plate of photomicrographs of thin sections under Polarised Light (PL), Cross-Polarised Light (CPL), CathodoLuminescence (CL) and Reflected Light (RL): a) Clear mono-crystalline quartz grain showing dissolution features at the borders. The mauve to pink coloured phases represent stained carbonate cements partly replacing the quartz. PL; b) Sub-angular quartz and sub-rounded feldspar grains coveded by a continuous clay coating (arrow) and showing different degrees of dissolution and replacement by carbonates (stained). In the picture centre are the relics of a feldspar grain nearly completely replaced. Note that the carbonates also precipitated as pore-filling phase plumbing the interparticle porosity. PL; c) Plagioclase grain affected by dissolution and replacement by carbonates (stained) in the grain centre as well as along the irregular borders. PL; d) Same in CPL. Note that the plagioclase grain was altered into clays (bright colours) before undergoing carbonate replacement; e) Sub-angular feldspar and quartz grains cemented by carbonates (stained). The quartz is not altered, whereas the feldspars show different degrees of alteration (more or less pronounced grey colour). PL; f) Same in CPL. The feldspars are possibly altered in kaolins showing vermicular texture; g) Black to reddish seams of organic matter run parallel to the bedding. PL; h) Sub-angular quartz and feldspar grains are coated by a continuous clay rim. PL.
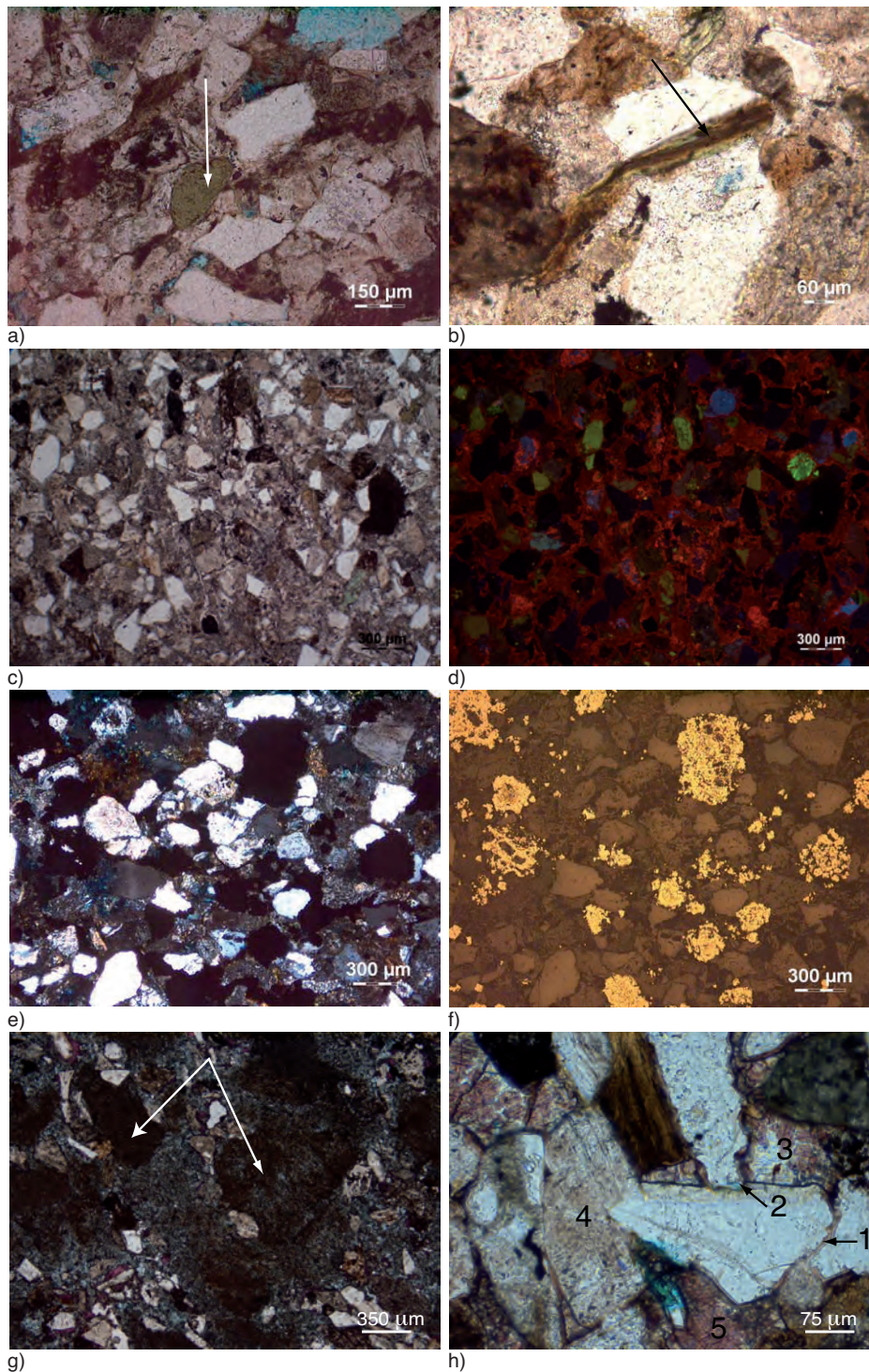
Figure 8

Plate of photomicrographs of thin sections under Polarised Light (PL), Cross-Polarised Light (CPL), CathodoLuminescence (CL) and Reflected Light (RL): a) Rounded grains of detrital chlorite (arrow) are found within sub-angular quartz and feldspar grains. PL; b) Diagenetic chlorite (arrow) replacing biotite grains and showing a greenish to brownish colour. PL; c) Typical field of view of the Mannville sandstones with quartz and feldspar grains replaced and cemented by carbonates. PL; d) Same in CL. The quartz and feldspar grains are blue to green luminescent to non-luminescent. The carbonates (both replacive and void-filling) show an uniform, unzoned and bright red luminescence. A brighter red luminescence corresponds to the borders and cores of the detrital grains replaced by carbonates; e) Framboidal pyrite possibly replacing organic matter. CPL; f) Same in RL; g) Mixed layer smectite/illite mineral (arrow), with a diffuse aspect, filling pore space; h) Typical field of view of an Upper Mannville sample showing 1- clay coating, 2- compaction feature and grains interpenetration, 3- quartz partial dissolution, 4- kaolinisation of feldspars, 5- calcite cement. PL.

R Deschamps et al. / Impact of Mineralogy and Diagenesis on Reservoir Quality of the Lower Cretaceous
Upper Mannville Formation (Alberta, Canada)

43

– *Kaolins*: Kaolins are always present in the studied samples in various amounts, and mostly corresponds to blocky kaolins. In the Upper Mannville sandstones, the observed authigenic kaolins derived from the replacement of detrital feldspars *(Fig. 7e, f)* and to a lesser extent micas.

Carbonate Cements

Carbonates form a significant diagenetic product in some samples of the Upper Mannville sandstones, both as pore filling and replacive phases. Carbonates are not ubiquitous, but when present, their proportion can reach up to 30% of the total rock volume *(Tab. 1)*. The observed carbonates include calcite, dolomite, ferroan dolomite (up to ankerite), and locally siderite:

– *Calcite*: Calcite (from ferroan to non-ferroan) is the most abundant carbonate phase. It occurs as blocky mosaic to poikilotopic cement filling the primary pore space *(Fig. 7a, c)*, and as replacement of grains like partly dissolved quartz, feldspars and volcanic rock fragments, occupying the secondary intraparticle pores *(Fig. 7b)*. Remnants of feldspars and quartz are usually preserved within the replacive calcite but locally the replacement can be complete. Pore filling calcite is volumetrically more abundant than replacive calcite. They both show a uniform, unzoned and bright red luminescence *(Fig. 8c, d)* suggesting a coeval origin from the same fluid;

– *Dolomite*: Ferroan dolomite is present in minor amounts. It has been observed only in few samples. Dolomite occurs generally as poikilotopic cement, usually stained in blue by potassium ferricyanide, but can also replace feldspar and less commonly quartz grains. In both cases the dolomite shows a bright red and uniform luminescence undistinguishable from the one displayed by the calcite phases previously described;

– *Siderite*: Siderite is quite abundant in these sandstones, and it occurs as intergranular pore fill cement, and as cement rims around detrital grains.

Others Authigenic Minerals

Other diagenetic minerals include pyrite and albite. These minerals are not abundant, and are distributed locally:

– *Pyrite*: Crystals of framboïdal pyrite are commonly found in small quantity in the Upper Mannville sandstones. The framboidal pyrite commonly replaces organic matter and corresponds to dark grains that appear golden yellow in reflected light *(Fig. 8e, f)*;

– *Albite*: Authigenic albite is present in most of the studied samples as replacement crystals on detrital potassic feldspars and plagioclases. It remains difficult to quantify the proportion of authigenic albite in the Upper Mannville fluvial sanstones as plagioclases are also present as detrital grains. Secondary pores generated by dissolution of K-feldspars and plagioclases are partly or completely filled by albite.

3.3 Oxygen and Carbon Isotope Composition of Carbonates

The O and C stable isotope analyses were performed on bulk samples with abundant carbonates (15-35%) and are summarised in Figure 9. The values are plotted together with those of Early Cretaceous seawater calcite (Veizer *et al.*, 1999). It derives that the analyzed carbonate phases are depleted in both ^{13}C and ^{18}O compared to the marine calcites which would have been precipitated from Early Cretaceous seawater during early diagenesis. The carbonate phases are therefore more correctly interpteted as the result of burial diagenesis.

The carbonates fall in a relatively large cloud characterized by $\delta^{18}O$ between –17 and –8‰, and $\delta^{13}C$ between –9 and 0‰ *(Fig. 9)*. With some exeptions, a very general trend towards more negative values of both parameters is associated to the samples which have suffered deeper burial conditions, *i.e.* samples from 01-19 and 13-27 wells, which accounted for more than 4 km of maximal burial.

It was possible to compare the isotope geochemistry of the studied samples with those reported in literature for the Alberta basin by Connolly *et al.* (1990). These authors furnished two main geochemical datasets for the Lower Cretaceous Ostracod and Glauconitic (Mannville Group), and Viking formations comparable to the Upper Mannville samples we studied. The former dataset includes temperature and oxygen isotope composition of the present-day connate waters hosted within these rock formations, whereas the latter dataset reports $\delta^{18}O$ and $\delta^{13}C$ of carbonates (including calcite, siderite and dolomite) found in the same rock formations as authigenic minerals. Results from both geochemical datasets relevant to this study were reported in Figure 9. It can be observed that most of the carbonate samples from the Upper Mannville have $\delta^{18}O$ values which fall within the field of calcites precipitated in equilibrium with present-day brines ($\delta^{18}O$ between –13.0 and –15.7‰; see the light yellow field in *Fig. 9*), whereas the two samples showing the higher $\delta^{18}O$ values fall within the field of dolomites in equilibrium with the same fluids ($\delta^{18}O$ between –7.5 and –10.8‰; see the light blue field in *Fig. 9*). Furthermore, the samples with more negative $\delta^{18}O$ are partially overlapped by those of authigenic calcites from the Ostracod, Glauconitic and Viking Fms. (see stars within the yellow line in *Fig. 9*), whereas those with less negative $\delta^{18}O$ are partially overlapped by authigenic dolomites and siderites from the same rock formations (see stars within the blue line in *Fig. 9*).

By analogy with the isotope composition reported for authigenic carbonates of known mineralogy by Connolly *et al.* (1990) it can be concluded that within the 15 bulk samples analyzed in this study, 13 were dominated by calcite and 2 by dolomite and ankerite. Nevertheless, the Upper Mannville

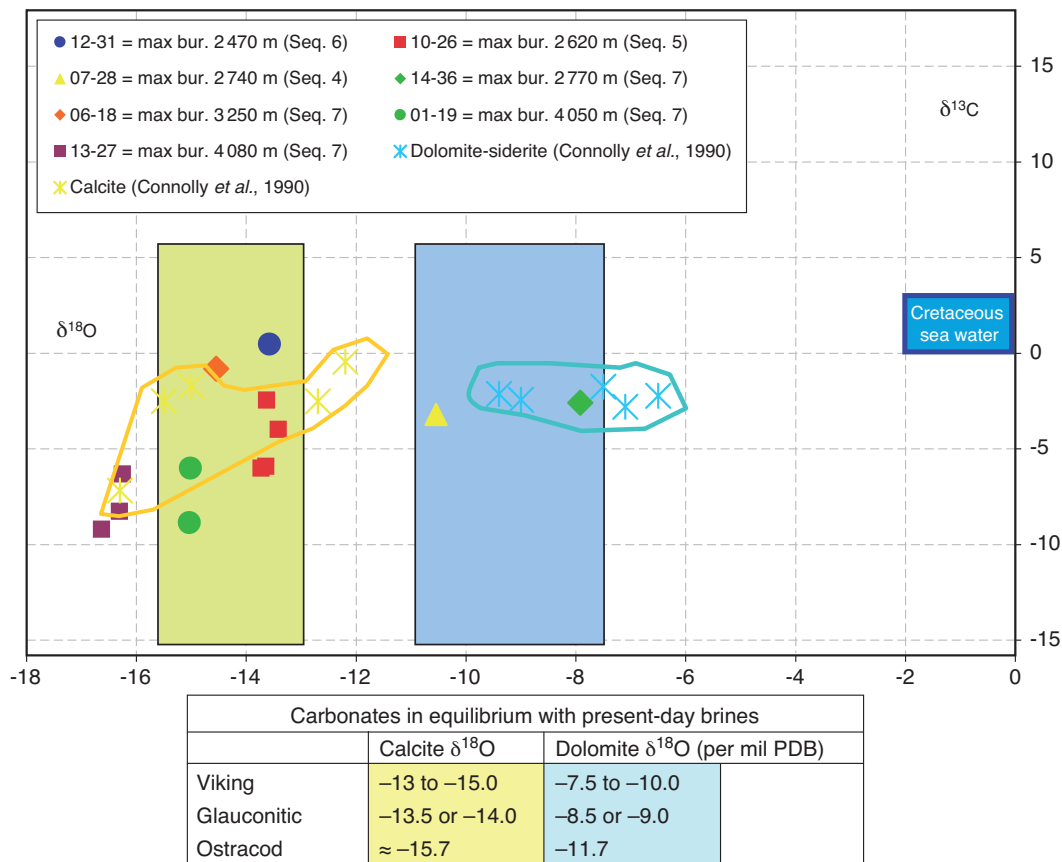| Carbonates in equilibrium with present-day brines		
	Calcite $\delta^{18}O$	Dolomite $\delta^{18}O$ (per mil PDB)
Viking	−13 to −15.0	−7.5 to −10.0
Glauconitic	−13.5 or −14.0	−8.5 or −9.0
Ostracod	≈ −15.7	−11.7

Figure 9

O and C isotope composition analyzed from bulk samples containing between 15 and 35% of carbonate phases. In the legend the stratigraphic position and the well of provenance of the samples are reported together with the maximum burial they have experienced. The more negative $\delta^{18}O$ and $\delta^{13}C$ values refer to the samples which underwent the maximum burial (*i.e.* 01-19 and 13-27). The values corresponding to the Lower Cretaceous seawater are reported in the blue frame (Veizer *et al.*, 1999). The oxygen isotope composition of calcite and dolomite cements which would precipitate in equilibrium with present-day brines are represented by the light yellow and light blue fields respectively; the values were derived from temperature and present-day brine oxygen composition from Connolly *et al.* (1990) by applying the fractionation equations of Friedman and O'Neil (1977) for calcites and of Land (1983) for dolomites. The data from calcite and dolomite-siderite cements from the Lower Cretaceous Ostracod, Glauconitic and Viking fms are contained within the yellow and the blue lines, respectively (values from Connolly *et al.*, 1990).

calcites seem to be richer in light carbon ($\delta^{13}C$ is most commonly less then −4.0‰) compared to those reported from Connolly *et al.* (1990) from equivalent rocks ($\delta^{13}C$ is most commonly above −2.5‰). This could suggest a slightly different source for the carbon of the carbonate mother fluids.
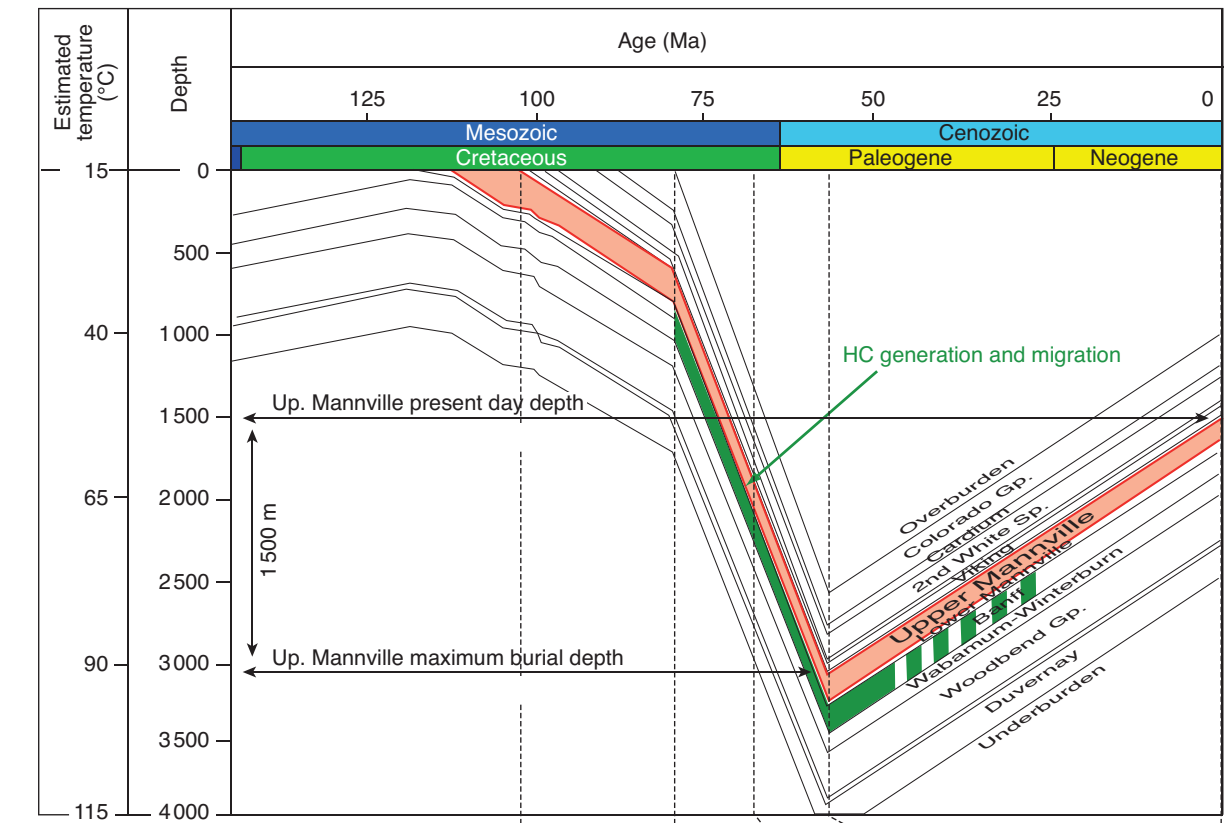
4 DISCUSSION

4.1 Diagenetic Evolution and Processes

4.1.1 Paragenesis

The mineralogy and the petrophysical properties of the Upper Mannville fluvial sandstone filling the incised valleys

have undergone significant diagenetic modifications (Euzen *et al.*, 2010, 2011). A paragenesis has been established, based on the textural relationships and paragenetic sequences reconstructed on seventy one thin-sections. In absence of datations, the diagenetic events described hereafter are ranked following a relative chronological order. A tentative correlation between the paragenesis and the WCSB basin evolution is nevertheless proposed in Figure 10.

The paragenesis is reconstructed in Figure 10b, and includes: a) Clay coating around detrital grains (chlorite, smectite) and siderite; b) Pyrite precipitation and replacement of organic matter; c) Chemical compaction and grains inter-penetration; d) Feldspars and quartz grains dissolution; e) Clay authigenesis (smectite-illite transformation, feldspars

Figure 10

Tentative correlation between the diagenetic events and the basin burial history with a) burial curve of the Western Canadian Sedimentary Basin in the studied area (modified from Higley *et al*., 2009); and b) paragenesis of the Upper Mannville Formation incised valleys sandstone infill.

kaolinitization), feldspars albitization; f) Carbonate cementation and replacement (calcite, ankérite and dolomite); g) Chloritization of micas and h) Carbonate cements partial dissolution:

a) Grain coating and pore lining clay minerals are the earliest authigenic clay minerals, and occur probably as chlorite, smectite, or mixed layer clays *(Fig. 8c)*, and siderite. The grain coation by clay minerals predates the grains interpenetration stage that occurs by compaction during burial;

b) Pyrite formation generally occurs very early during the diagenetic history, replacing organic matter (Berner, 1984). Pyrite is rare in thin-sections, and shows generally a patchy distribution. Framboidal pyrite is identified in several samples. Optical microscopy XRD and SEM analysis confirm the presence of pyrite crystals ranging from 50 to 200 μm in the studied sandstone;

c) Chemical compaction is the third diagenetic event for the Upper Mannville fluvial sandstones. Grain interpenetration features are commonly observed within these sandstones *(Fig. 8e)*. This results into a reduction of the primary porosity and ductile minerals (detrital clay minerals *e.g.* smectite and locally mud-clasts) smering in the pore space;

d) Detrital grains dissolution then occurred, predating clay minerals authigenesis. Feldspars grains (both K-feldspars and plagioclases) are partly to completely dissolved and replaced either by kaolins or by albite *(Fig. 7c, d, g, h)*. Quartz grains show less dissolution than feldspars because of their best stability. Aggressive acidic waters may be involved in the framework grains dissolution process. The inferred waters might have a meteoric origin, enriched in organic-rich particles, coming from the abundant coal deposits within the Upper Mannville Formations. Meteoric waters percolating through coal or peat usually become strongly acidic due to the presence of CO_2 and organic acids produced during microbial alteration of organic matter. These acidic meteoric waters favor the dissolution of silicates grains (*e.g.* feldspars, quartz and micas) (Marcelo and Ketzer, 2002). These organic acids have the potential to exert a significant influence on silicate minerals reactions in natural systems by accelerating dissolution rates (Blake and Walker, 1999);

e) Clay minerals precipitation and transformations are clearly linked to the previous diagenetic stage, and mainly concern illite formation through the smectite/illite transformation, and the kaolinitization of feldspars. Albitization of feldspars also occurred;

f) Carbonate cementation occurred almost at the same time or a bit later than the clay minerals transformations cited previously;

g) Chloritization of biotite in the most deeply buried samples;

h) Carbonate cement partial dissolution.

4.1.2 Authigenesis

Diagenesis of sandstones is dependant in the first place on detrital mineralogy, sediment texture, organic content and initial pore water chemistry, and these factors are largely controlled by sediment source and depositional environment (De Ros *et al.*, 1994; Worden and Burley, 2003). Maximum burial depth, thermal history as well as fluid chemistry and circulation ultimately control the diagenetic evolution through time (Worden and Burley, 2003). The authigenesis of pyrite, illite, kaolins, albite, carbonates and chlorite is discussed in the next sections.

Clay Coating

Continuous grain coating of clays is observed on most of the studied samples. Among various types of clay coating described in the literature (Aase *et al.*, 1996; Ehrenberg, 1993; Pittman *et al.*, 1992), chlorite is the most frequently described. In our case, the detrital grain coating is constituted by chlorite and/or smectite and siderite minerals, forming crystals perpendicular to the detrital grains. Presence of radial coating around grains indicates early stage of authigenesis, in association with pedogenic processes (Walker *et al.*, 1978). The presence of abundant coating suggests that a precursor clay mineral was present in the depositional environment (Ehrenberg, 1993). Smectites and chlorites were probably the most abundant clay minerals present in this system. Warm to temperate climate prevailed during Barremian to Albian times in North America (Hallam, 1985), favouring smectites formation (Gradusov, 1974; Rateev *et al.*, 2003) more than other clay minerals. The alteration of igneous and metamorphic minerals (*e.g.* micas) in the sedimentary system, originated from the erosion of the mountain range westward also favoured detrital Fe-rich clay minerals precursors and chlorite formation (Grigsby, 2001). Clay rims may thus formed during eodiagenesis linked with pedogenic processes (Walker *et al.*, 1978) as it was present in the sediment during sandstone deposition, and predates all other diagenetic phases, including compaction and detrital grains interpenetration *(Fig. 8c)*.

Crystals of pyrite found in the fluvial deposits of the Upper Mannville incised valley fill are interpreted as being a product of the degradation of organic material under reducing conditions (Berner, 1984; Butler and Rickard, 2000). Organic material was abundant during lower Cretaceous Mannville deposition, as thick coal layers are commonly found in the floodplain and coastal plain deposits, constituying the host deposits of the incised valley systems formed during lowstand periods (Deschamps *et al.*, 2008).

Authigenesis of Clay Minerals

Fluvial sandstones of the Upper Mannville are dominated by illite-smectite, with subordinate amounts of kaolins and pore filling chlorites. Percolation of gravity-driven acidic meteoric waters may have activated the dissolution of the most unstable detrital minerals (*e.g.* feldpars and micas), starting

shortly after deposition (Weaver, 1989). The feldspars, micas and quartz dissolution process provide potassium, calcium, magnesium, iron and silica in the pore water system, enable mineral replacement and precipitation.

– *Authigenic kaolins*: Authigenic kaolins occur mainly as feldspars (plagioclases and K-felspars) and micas (muscovite) replacements. According to Hancock (1978) and Hancock and Taylor (1978), kaolin crystallisation is promoted at shallow burial depth by meteoric fluids that flush the formation during shallow burial early telogenesis. As a consequence of K-feldspars dissolution, kaolins precipitates according to:

$$\text{Feldspar} + 2H^+ + 9H_2O \rightarrow \text{Kaolins} + 4H_4SiO_4 + 2K^+$$
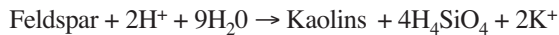
The meteoric fluids required for the K-feldspar alteration and subsequent kaolins precipitation need to be also CO_2-rich or organic acid-rich, according to Lanson *et al.* (2002) and Ehrenberg *et al.* (1991). These acidic fluids may result from the migration of hydrocarbons expelled from mature Devonian and Mississippian source rocks that reached the oil window in the foothills during the Late Jurassic/Lower Cretaceous (Schneider, 2003; Faure *et al.*, 2004);

– *Illite smectite mixed layer clays (I/S)*: The mixed layer smectite/illite mineral is an intermediate product of reaction involving pure smectite reacting to form illite. This reaction is known to be strongly controlled by temperature (Perry and Hower, 1972; Hower *et al.*, 1976). Experimental studies have evidenced that the smectite/illite reaction occur in the sedimentary basins during burial when temperature reach 60°C (Freed and Peacor, 1989). However, numerous studies have also established that for the transformation to proceed from smectite to illite, the presence of potassium ions is required to initiate and allow this reaction (Meunier, 2005). According to Meunier (2005), once the reaction initiated, smectite progressively transforms into illite following two main steps:
• randomly ordered I/S minerals with 100% to 50% smectite ($R = 0$),
• ordered I/S minerals with 50% to 100% illite ($R = 1$). Pure smecite and pure illite are the end members of this reaction.

In our case, twenty two samples have been analyzed with XRD. These samples have been taken at different depths in 5 wells, to assess the mineralogical composition variations according to depth. The diagram in Figure 11a shows the variation of I/S minerals evolution as a function of the depth. The clay mineral diffraction pics measured on both wells 14-36 and 10-26, which samples were taken at a present day depth of –1 250 m Measured Depth (MD),
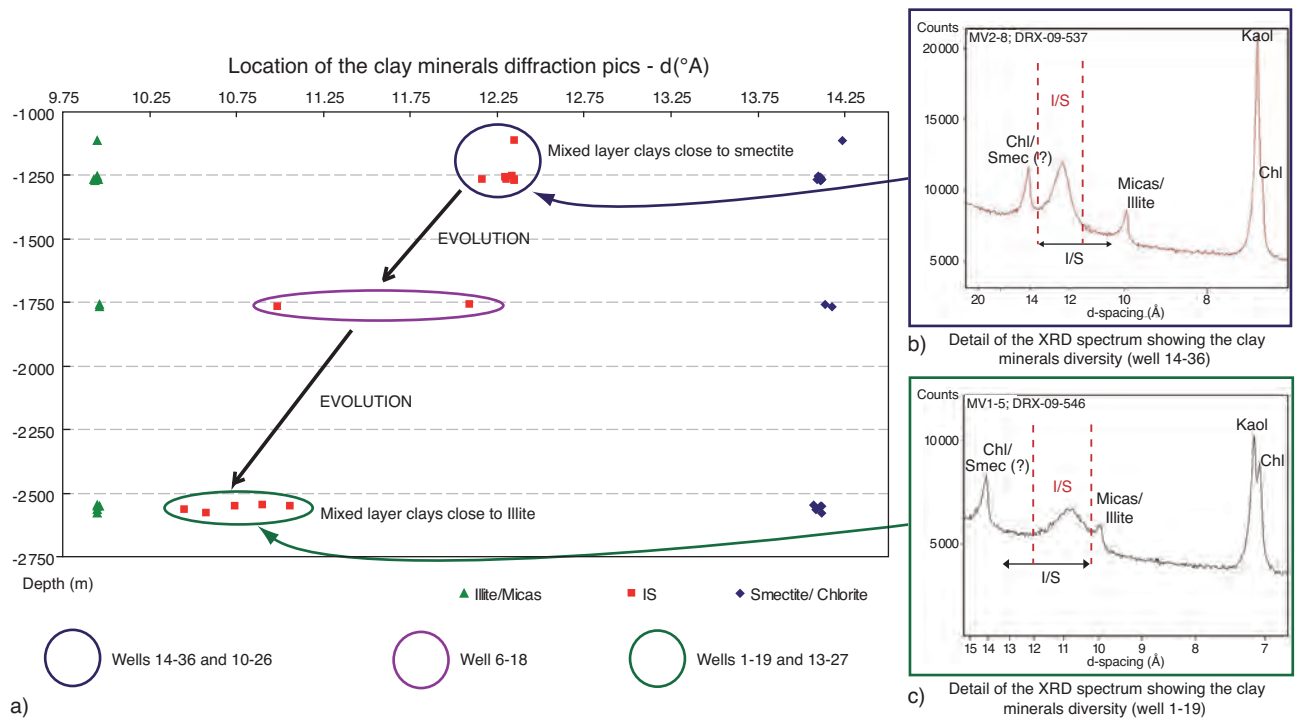

Figure 11

Evolution of the nature of the mixed layer clay minerals (I/S) as a function of depth, using XRD analysis, and location of diffraction raies of mixed layer clay minerals (I/S), smectites and illites related to the depth.

correspond in the diffractogramm Figure 11b to a peak close to the smectite end member peak. These clay minerals correspond to randomly ordered I/S minerals. Samples taken on the well 6-18 at a depth of 1 750 m present day show more dispersed values, suggesting a displacement of the peak towards the illite end member values. Another set of samples taken from two wells (1-19 and 13-27) taken at a present day depth of 2 550 m (MD) show a pic corresponding to ordered I/S, corresponding to ordered I/S minerals close to the illite end member values *(Fig. 11c)*. This analysis evidences the variations of I/S clay minerals structure and composition as a function of the depth, which is directly linked with temperature. On the diffractogram, the pic corresponding to I/S clay minerals moves from the smectite end member peak towards the illite end member pic as the depth and temperature increase.

According to the smectite/illite balance equation described by many authors (Eslinger and Pevear, 1988; Meunier and Velde, 2004), a simplified equation of transformation is proposed hereafter:

$$Smectite + K^+ \rightarrow Illite + Si^{2+} + Mg^{2+}$$
$$+ Fe^{2+} + Ca^{2+} + Na^+ + nH_2O$$
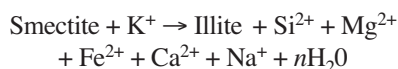
The potassium needed to allow the smectite-illite transformation can be supplied by the dissolution and transformations of different K^+ rich detrital minerals. Four main potassium sources may be involved: potassic feldspars dissolution, kaolinitization of felspars (see section above), chloritization of biotites and feldspars albitization release K^+ cations in the pore water system. These reactions are observed as occurring contemporeanously in the Upper Mannville paragenesis *(see Fig. 10b)*.

Albitization of feldspars can also contribute to the release of cations involved in authigenic minerals precipitation. Both K-feldspars and plagioclases have been identified in the samples, but their relative proportions have not been precisely counted, even if the proportion of plagioclases seems to be greater than K-feldspars. After Morad *et al.* (2000) and Saigal *et al.* (1988) albitization may start at temperature around 65°C.

The K-feldspars albitization also release K^+ cations in the pore system, and the reaction can be expressed as follow (Aagaard *et al.*, 1990):

$$K \, feldspar + 2Na^+ \rightarrow albite + 2K^+$$
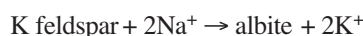
A source of Na^+ ions is required to allow this reaction, and Na^+ ions can be supplied by plagioclase dissolution, which releases Na^+ and Ca^{2+} ions in the pore system, as well as the transformation of smectite into illite, which releases sodium ions as a precursor for albitization (Van de Kamp and Leake, 1996);

– *Authigenic chlorite*: Authigenic chlorite occurs as mica replacement. The micas originally presents as detrital minerals mostly correspond to biotite, and to a minor amount of muscovite. A simplified equation of transformation of biotite into chlorite is proposed hereafter (modified from Claeys and Mount, 1991):

$$Biotite \rightarrow Chlorite + K^+$$

Alteration of micas (*e.g.* Biotite) with increasing temperature is not a major reaction observed in the Upper Mannville samples, but contributes anyway in the K^+ ions release that helped the smectite transformation into illite.

Authigenesis of Carbonate Phases
Carbonate authigenesis in the Upper Mannville incised valley fill includes the emplacement of both replacive and cement mineral phases possibly corresponding to a unique diagenetic fluid event. The carbonates are found replacing quartz and feldspar grains (replacement origin). They can also form a cement filling intergranular pores as well as the intragranular dissolution porosity. The overall effect of the carbonate authigenesis is to reduce the primary as well as the secondary porosity. It is therefore crucial to determine carbonate fluid origin and timing to better predict the distribution of porous reservoirs within the Upper Mannville Fm.

It can be excluded that the carbonates were originated from marine fluids during early to shallow burial diagenesis because neither the oxygen nor the carbon isotopic signatures of the carbonates reflect those typical of a marine fluid dictated diagenesis; both $\delta^{18}O$ and $\delta^{13}C$ are indeed more negative compared with the stable isotope signature of Cretaceous sewater *(see Fig. 9)*. Thus, the carbonates were possibly the result of burial diagenesis. The calcium necessary for carbonate precipitation was possibly derived from feldspar alteration in the burial environment according to the reaction:

$$2(Na,Ca)AlSi_3O_8 \rightarrow 2NaAlSi_3O_8 + 2Ca^{2+}$$
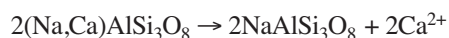
The origin of the fluids responsible for carbonate replacement and precipitation can be inferred from the oxygen and carbonate isotope geochemistry *(Fig. 9)*. The more negative $\delta^{18}O$ values in carbonates from samples having experienced the deepest burial conditions is in agrement with carbonates precipitated at higher temperatures during burial. Nevertheless, this shift towards lower $\delta^{18}O$ values could also be due to different fluid isotopic composition. It was possible to roughly estimate the $\delta^{18}O_{SMOW}$ of the carbonate mother fluids by integrating the isotope composition of the analyzed samples with their possible range of precipitation temperatures. In Figure 12 the fractionation equations of Friedman and O'Neil (1977) and Land (1983) were used to calculate the $\delta^{18}O_{SMOW}$ composition of fluids in equilibrium with calcites and dolomites, respectively. For each analyzed carbonate sample the $\delta^{18}O$ was plotted against its maximum burial temperature. The latter was calculated from the maximum burial depth of each sample (Higley *et al.*, 2009) by assuming a

R Deschamps et al. / *Impact of Mineralogy and Diagenesis on Reservoir Quality of the Lower Cretaceous Upper Mannville Formation (Alberta, Canada)*
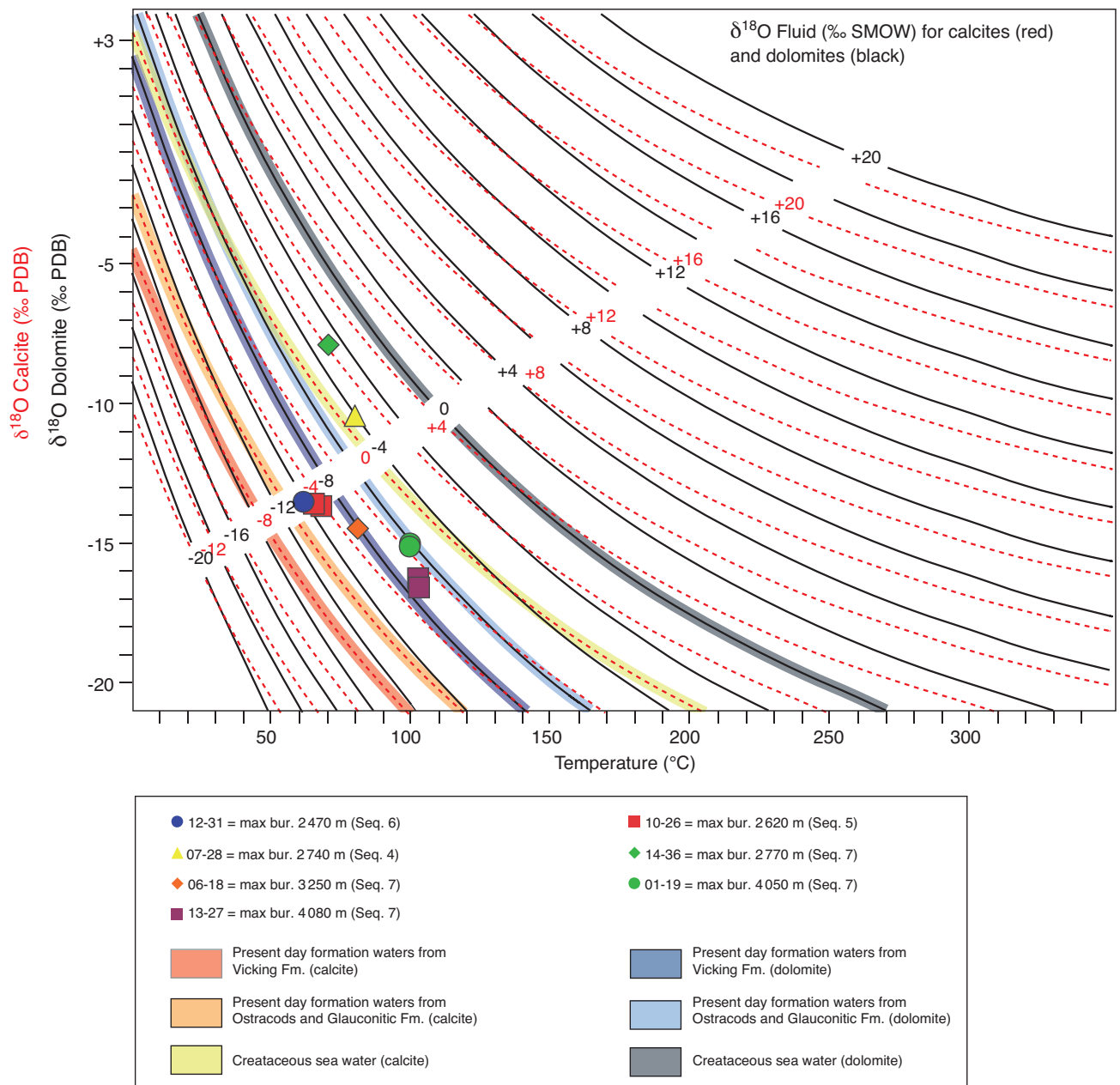
49

Figure 12

Precipitation temperature *versus* O isotopic composition of the carbonate phases analyzed. The fractionation equation of Friedman and O'Neil (1977) and Land (1983) were used to calculate the $\delta^{18}O_{SMOW}$ composition of fluids in equilibrium with calcites (dotted red curves) and dolomites (continue black curves), respectively. For each analyzed carbonate sample the $\delta^{18}O$ was plotted against its maximum burial temperature by assuming a constant geothermal gradient of 25°C/km throughout the Cenozoic. The differently colored fields refer to the $\delta^{18}O_{SMOW}$ composition of present-day formation waters from various Cretaceous formations (Connolly *et al..* 1990) and the composition of Cretaceous seawater.

geothermal gradient of 25°C/km. On the diagram the differently colored fields refer to the $\delta^{18}O_{SMOW}$ composition of present-day formation waters (Connolly *et al.*, 1990) and Cretaceous seawater.

It results that the Mannville carbonates were formed by fluids having $\delta^{18}O_{SMOW}$ in the range −6 to −2‰ for calcite dominated samples and in the range −4.5 to −3‰ for dolomite dominated samples. By taking temperatures lower

than those of peak burial, the $\delta^{18}O_{SMOW}$ calculated for each carbonate sample would shift towards even more negative values (refer to *Fig. 12*). These fairly negative values are typical of dilute meteoric fluids depleted in ^{18}O. It is suggested that the investigated carbonates formed subsequent to a pervasive influx of meteoric fluids through the WCSB which eventually mixed with original heavier formation waters. This is an important statement since it allows to broadly constraining the timing of the carbonate phases to the Cenozoic, *i.e.* after the uplift of the Canadian Cordillera had already started. To allow a flux of meteoric derived fluids within the studied buried foreland, the orogen in the West should have been already largely exposed in order to account for a large recharge area for meteoric fluids. Furthermore, the high relief of the emerging Canadian Cordillera could have caused a topographic barrier for atmospheric circulation, increasing rainfall and, in turn, meteoric water supply to the hydrogeological system. The important relief of the orogen may have thus justified a hydraulic head high enough to allow surface waters to penetrate deep into the Mesozoic succession of the coeval foreland basin. Bachu (1999) already described a basin scale flow system present in the southern part and the central part of the Alberta basin. The flow is driven by basin topography from recharge areas where aquifers crop out at high elevations in the foothills to the West to discharge areas at lower elevation in the basin. Schneider (2003) and Faure *et al*. (2004) also performed basin modelling to reconstruct the time evolution of the foreland basin in order to make quantitaive predictions of geological phenomena leading to hydrocarbon accumulations. Through the modelling, they both evidenced that the Lower Cretaceous strata were subjected to water flowing towards the North-East and originated from the foothills, with a contribution of South-East flowing water in the eastern edge of the basin where the Lower Cretaceous strata were exposed.

Such a model has analogies with the "topography-driven model" by Garven and Freeze (1984) which invokes as driving flow mechanism in belt-foreland systems the gravity effect due to topography differences between orogen and foreland. This model is also in agreement with the accepted interpretation of the present-day formation waters stored within the foreland buried succession. The present fluids are considered to be obtained by a mixing between meteoric and formation waters and became isolated from present-day meteoric recharge during the Pliocene (Longstaffe and Ayalon, 1987; Connolly *et al*., 1990). Interestingly, the oxygen composition of the fluids found at present in the reservoirs is similar to the one of the fluids precipitating past carbonates (refer to *Fig. 10, 13*), this suggesting a quite stable hydrologic system throughout the Cenozoic.

The negative $\delta^{13}C$ values recorded in the Mannville carbonate samples *(Fig. 9)* allow to validate and improve the proposed model. There are three main possible sources for light ^{12}C in carbonate cements (Morse and MacKenzie, 1990):

– Kerogen contained within organic rich source rocks undergoes maturation during burial and releases abundant CO_2 together with water and hydrocarbons. CO_2 is very soluble in water and have the potential to be fixed within the nearby reservoir rocks as carbonate cement;

– CO_2 can be also produced by the biodegradation of oil and gas and fixed in carbonate phases;

– The third process which can explain slightly negative $\delta^{13}C$ of carbonates is the incorporation of light ^{12}C by a surface meteoric fluid which penetrates at depth passing through soils in which light CO_2 is commonly liberated by the oxidation of organic matter (Morse and MacKenzie, 1990).

The previous discussion on the possible origin of the fluid-flow would suggest the flush of meteoric waters through the basin due to the meteoric recharge as the most probable hypothesis to explain the negative $\delta^{13}C$ of the Mannville carbonate samples. Nevertheless, the carbonates from the Upper Mannville display a more negative $\delta^{13}C$ signature compared to other carbonate cements from literature (refer to *Fig. 9*). Therefore, it is possible that a second component of light ^{12}C was derived by a source different than the meteoric fluid.

The hypothesis that the light carbon partially derived from the biodegradation of hydrocarbons migrated through the Mannville Fm. has to be ruled out since carbonates containing carbon of such an origin commonly have much more negative $\delta^{13}C$ (down to $-30‰$; compare to Irwin *et al*., 1977; Dimitrakopolous and Muehlenbachs, 1987).

The hypothesis that the light carbon partially derived from the organic acids produced by the maturation of organic matter within the Mannville during burial better fits to the reported $\delta^{13}C$ values (compare with Macaulay *et al*., 1998, 2000). Some evidence supporting this hypothesis comes from the temperature-$\delta^{13}C$ relationship encountered in the studied samples *(Fig. 9)*: the higher the temperature experienced by the host rock the more carbon was produced by organic matter maturation, which is reflected in the most deeply buried samples from the wells 01-19 and 13-27.

In conclusion, the presented data support an origin for the carbonates (both replacive and cement phases) during the Cenozoic as due to the flux of meteoric fluids in the deep subsurface of the foreland and mixing with formation waters, triggered by a meteoric recharge located in correspondence of the orogen in the West. A minor component of light ^{12}C was possibly derived from the maturation of the organic matter contained within the Upper Mannville.

4.2 Quantification of Diagenetic Phases

The quantification of diagenetic phases consists in estimating the proportion of mineralogical phases appearing and
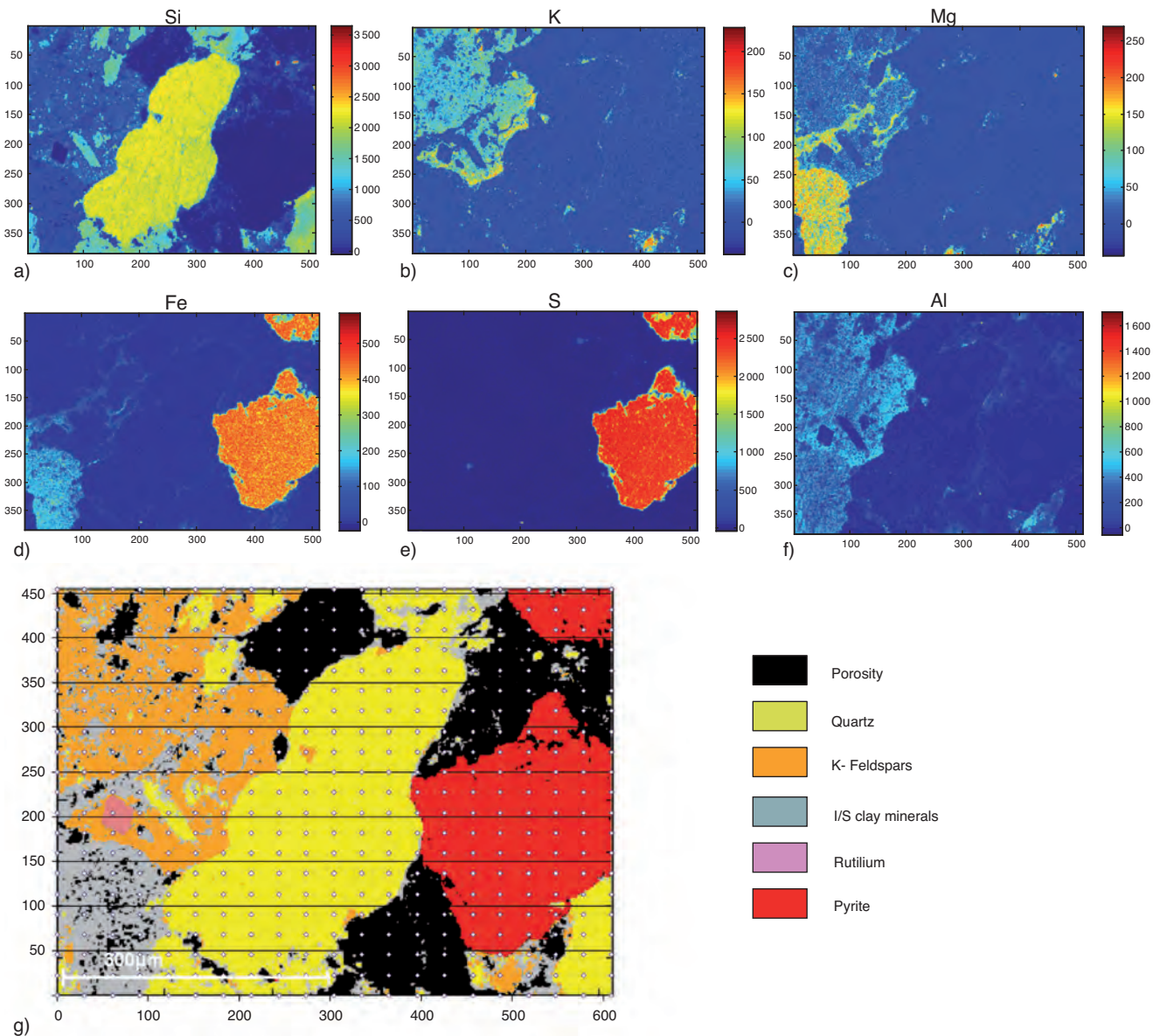
Figure 13

Spectral analysis and mineral mapping of the sample 13-27 resulting from 200 000 "quick" analysis and a matrix of 441 standardised analysis to obtain the major elements composition of the sample, with a) Silicium, b) Potassium; c) Magnesium; d) Iron; e) Sulfure; f) Aluminium. g) The mineral mapping is obtained by a statistical cluster analysis.

disappearing, based on the paragenesis defined in this study. Mineral mapping was performed on a few representative samples using a SEM-based punctual chemical analysis method. Backward reconstruction of dissolutions and cementations from 2D mineral maps was used to quantify the evolution of visible porosity through time.

Two representative samples have been selected to illustrate the method used for quantifying the diagenetic phases. The selection has been made according to the sample representativity of the whole set of samples used for this study.

The first sample corresponds to a clay mineral-rich arkose, without carbonate cement filling the pore space (well 13-27). The second sample is a carbonate cement-rich arkose, with very low clay mineral content (well 01-19). They are both representative of the studied Upper Mannville samples in terms of minerals occurence and proportions, as we observed

that the carbonate cements were poorly developed in the samples rich in clay minerals (*e.g.* interstratified minerals).

4.2.1 SEM Analysis and Mineral Mapping

The results of this numerical process are the identification of minerals at location on the map *(Fig. 13)*. The chemical mapping is displayed on top of Figure 13a-f; the mineralogical map obtained from the cluster analysis is shown in Figure 13g. The white dots on the mineralogical map correspond to the punctual analysis (step = 30 μm). The coherencies of the results obtained from "cartographic" analysis and from the "classical" punctual analysis have been cross-checked.

4.2.2 Quantification of Diagenetic Phases

The characterization of both detrital and authigenic minerals in the samples allow the material balance quantification in terms of both mineralogical and visible porosity changes during the diagenetic history. Starting from the reconstructed original texture and mineralogy, we quantified the porosity changes induced by the main stages of the paragenesis that induced a porosity variation for this sample (dissolution - precipitation stages) for both analyzed samples.

From the present day picture given by the spectral analysis and the mineral mapping, and by the integration of the authigenesis and dissolution stages defined in the paragenesis, we were able to reconstruct the sample texture at each step of the paragenesis, involving mineral transformations, porosity creation by dissolution and porosity destruction by cementation. The final step results in reconstructing the original texture and mineralogy of the rock. This method has been applied to both representative samples presented in Figures 14 and 15.

The sample 13-27 *(Fig. 14)* presents a final texture with quartz and feldspars (plagioclase) grains partly dissolved and replaced by clay minerals, and altered clay grain *(Fig. 15a, b)*. Pyrite is also present, but do not show any alteration features. The porosity calculated on the 2D picture reaches 19% of the total picture surface:

– *Step 1*: We assume by following the paragenesis backward that the last diagenetic stage that occured corresponds to the partial secondary pore space infill by clay minerals (phase 5 of the paragenesis, *Fig. 10b*). The clay minerals partially filling and replacing both quartz and feldspars grains have been removed *(Fig. 14c)*, and the porosity at this stage of the paragenesis was calculated at 28.7%. The porosity reduction due to clay mineral transformation and replacement reaches 9.7% in this sample;

– *Step 2*: The diagenetic stage that occurred before the stage 5 of the paragenesis corresponds to quartz and feldspars dissolution, and it was assumed that the secondary porosity observed in both quartz and feldspars grains in this sample was related to this stage of the paragenesis (stage 4, *Fig. 10b*). By removing the secondary porosity, we restored what most probably was the original texture of this sample *(Fig. 14d)*. The porosity in the original sample is estimated

at 15.6%, by removing the secondary porosity created during quartz and feldspars dissolution, so a porosity enhancement of 13.1%.

While restoring the texture and the mineralogy of the rock, we took into account the main diagenetic phases that strongly impacted the porosity. We neglected the effect of compaction/grains interpenetration, and the mineral volume changes during the smectite-illite transformation because of the complexity of assessing and quantifying their real effects on the rock texture and the porosity variations.

The same method was applied to the sample 1-19. This sample corresponds to a carbonate cemented arkose, with a large amount of plagioclases and potassic feldspars. Siderite, chlorite and pyrite grains are also present in smaller proportions *(Fig. 16a, b)*. Kaolins have been identified as feldspars partial replacement. The porosity of this sample is less than 2%, and probably corresponds to the last stage of carbonate cement partial dissolution (step 8 of the paragenesis, see *Fig. 10b*):

– *Step 1*: To restore the sample texture before the last diagenetic stage of carbonate cement partial dissolution, the secondary porosity induced was removed. The resulting texture corresponds to a completely cemented arkose, with no porosity left *(Fig. 15c)*;

– *Step 2*: The carbonate cementation and replacement that completely filled the pore space have then been removed to reconstruct the sample texture before this diagenetic stage *(Fig. 15d)*. The visible porosity before carbonate cementation is 41.8%;

– *Step 3*: The diagenetic stage strongly affecting the porosity that occured before the carbonate cementation and replacement stage is the quartz and feldspars dissolution (stage 4 of the paragenesis). We observed on the sample *(Fig. 15)* that quartz, feldspars and siderite grains are partly dissolved. By analysing the SEM image, it was possible to restore the initial grains shapes because of the presence of silica and iron faint traces where the grains were dissolved. After reconstructing the original grains shapes, we obtain what probably was the original texture of this sample, without taking into account the compaction effect. The initial porosity was 27.5%, with an enhancement of 14.3% by dissolution of quartz, feldspars and siderite grains.

The diagenetic phases quantification was performed on 2D thin sections, which do not really represent the real 3D aspect of the rocks.

4.3 Controls on Reservoir Quality

Reservoir quality is here defined as the amount of visible porosity measured on 2D thin-sections. In the Upper Mannville sandstones, the evolution of the reservoir quality through time is controlled by the initial mineralogy and
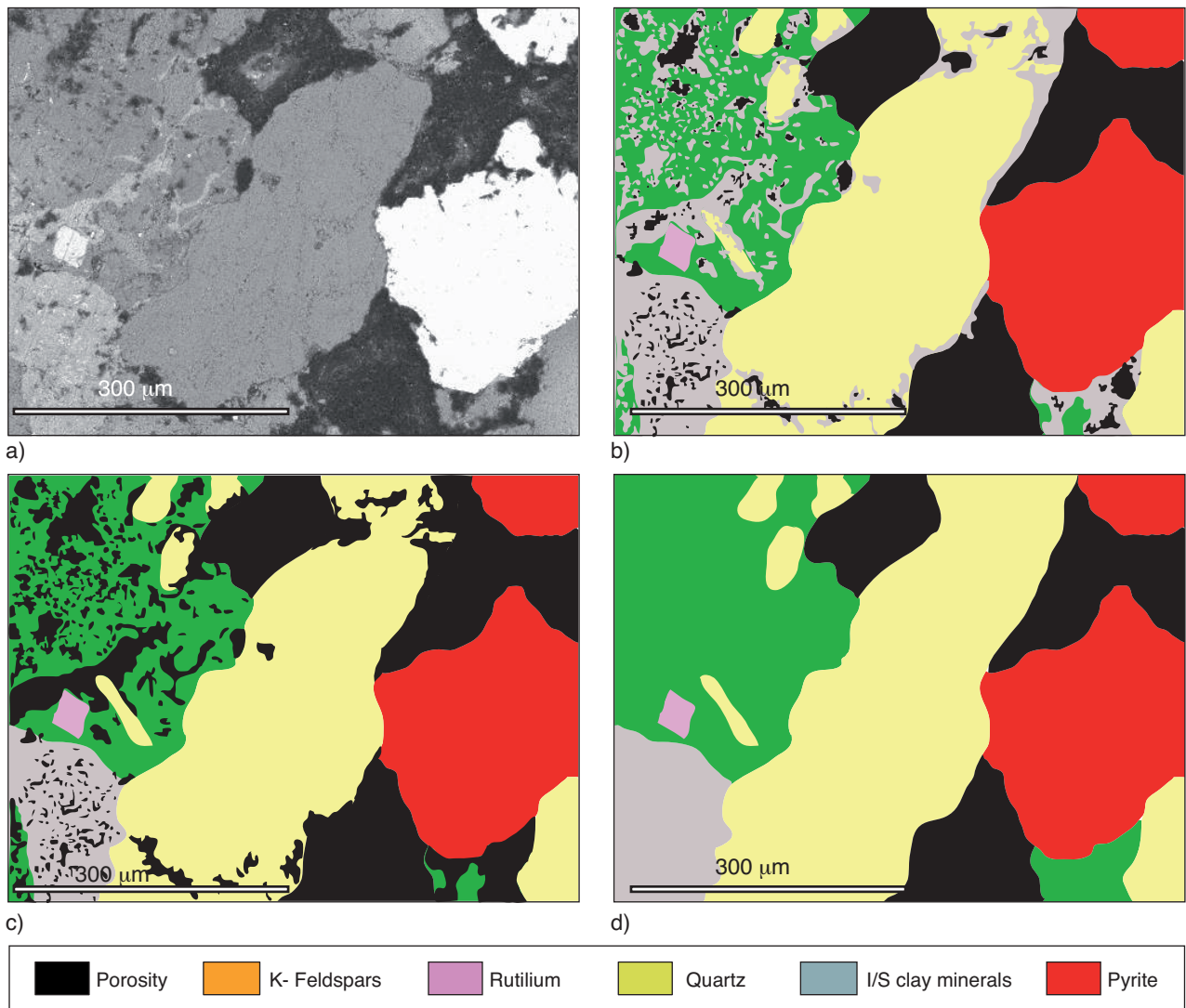
| ■ Porosity | ■ K- Feldspars | ■ Rutilium | ■ Quartz | ■ I/S clay minerals | ■ Pyrite |

Figure 14

Reconstruction of the texture and mineralogical composition of the sample 13-27 through the main diagenetic stages that strongly modified both mineralogical composition and apparent porosity: a) SEM picture of the sample; b) Mineral mapping of the sample; c) Texture before the quartz and feldspars replacement by clay minerals (*e.g.* kaolins); d) Texture before the quartz and feldspars dissolution diagenetic stage, that closely corresponds to the initial texture of the rock.

texture and the dissolution and cementation events that occurred during diagenesis. The initial proportions of quartz, feldspars and clay minerals initially present will impact the diagenetic processes and ultimately the evolution of the reservoir quality.

A negative correlation is observed between the amount of clay minerals present in the studied samples (*e.g.* mixed layer clay minerals and kaolins) and the abundance of carbonate cement *(Tab. 1)*.

A negative correlation between the amounts of quartz/feldspars and carbonate cement is notable in the Upper Mannville reservoir samples. The proportion of carbonate

cement is more important when the amount of both quartz and feldspars is low (less than 50% of the sample).

Carbonate cementation and replacement appears to be the most destructive process of reservoir quality, whereas the role of siderite and dolomite is less certain.

Impact of Clay Minerals
The abundance of clay minerals inhibates extensive carbonate cementation. In the studied samples, the minimum quantity of carbonate cements is observed when the total clay content reaches 15 to 20% of the rock volume. The carbonate cementation is the most extensive when the amount of clay minerals is less than 10% and the visible porosity left in this
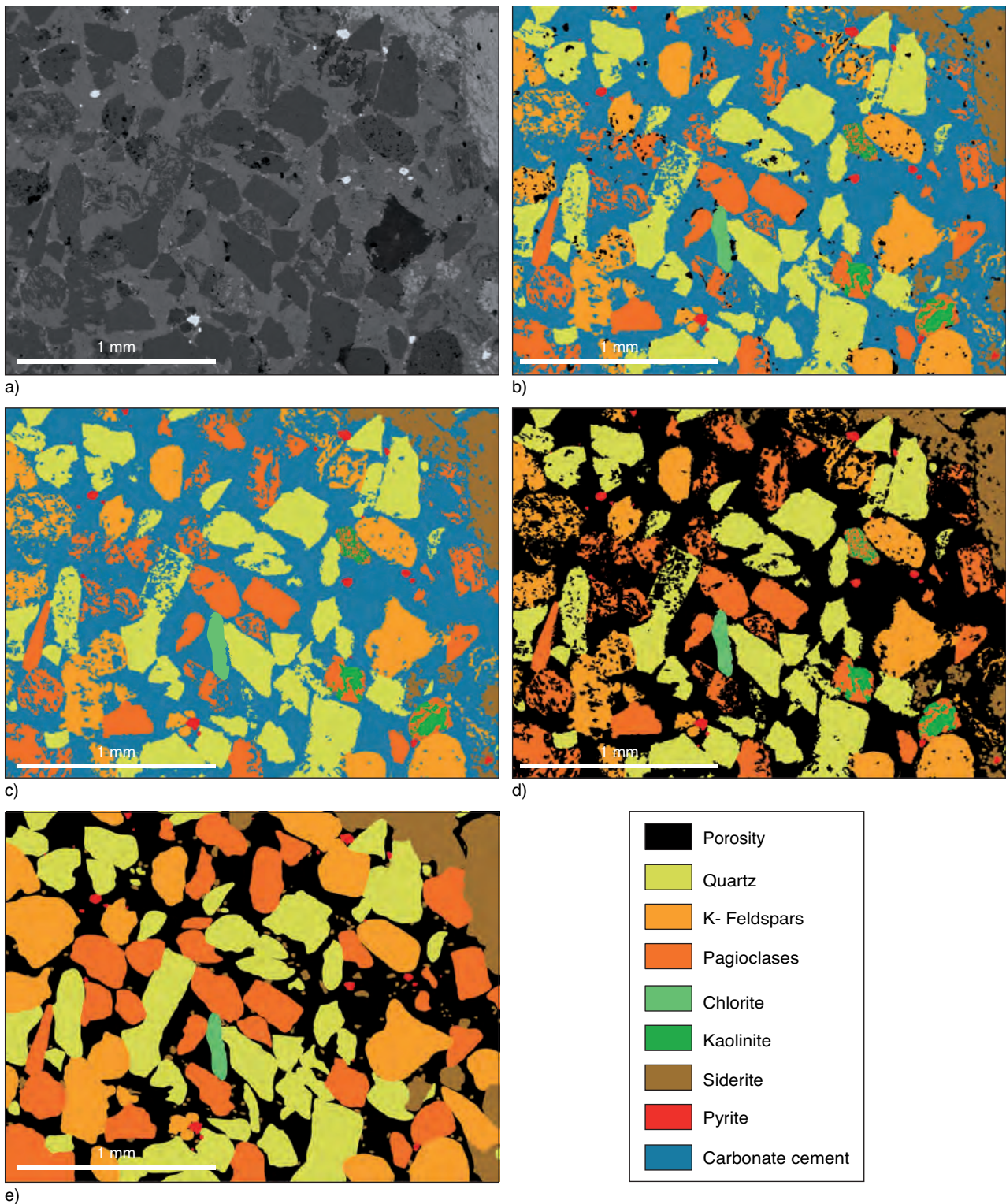
Figure 15

Reconstruction of the texture and mineralogical composition of the sample 01-19 through the main diagenetic stages that strongly modified both mineralogical composition and apparent porosity: a) SEM picture of the sample; b) Mineral mapping of the sample; c) Texture of the sample before the last diagenetic stage of carbonate cement partial dissolution; d) Texture of the sample before the carbonate cementation and replacement diagenetic stage; e) Texture of the sample before the quartz and feldspars grains dissolution stage, that closely corresponds to the initial texture of the rock.

case never reaches more than few percents. The most probable reason to explain such negative correlation is the absence of good permeabilities for fluid flow, due to the presence of clay minerals that might plug the pore throats, preventing the meteoric fluids responsible for carbonate cementation to flow in clay-rich parts of the reservoirs.

The effect of smectite/illite transformation remains more difficult to assess, because its impact on porosity changes will depend on several parameters. We observe a volume decrease between the initial smectite and resulting quartz/illite. The consequence on porosity is also linked to the permeability and the mechanical constrains. The porosity decrease linked to the mechanical compaction could be reduced by the ability to drain the produced water during illitisation at low permeability. In this case, the porosity variation might be linked to the hydraulic fracturation. On the contrary, if permeabilty allows efficient water drainage, porosity can follow a compaction law which will be linked to the effective stress and mechanical properties of the rocks.

In our case, the negative correlation between carbonate cements and proportion of clay minerals suggests that permeability of clay-rich reservoir rocks is not efficient enough for CO_2-rich water to flow. But the absence of over-pressured reservoirs shows that the water produced by illitisation could be drained. In addition, the kinetics of mineral transformation (illitisation and carbonate cementation) are very contrasted. Carbonate precipitation is a faster phenomenon than illitisation. The presence of a certain amount of mixed layer clay minerals may prevent from extensive carbonate cementation, but the compaction effect may significantly reduce the reservoir quality at depth.

Impact of Quartz and Feldspars Dissolution
Dissolution of quartz and feldspars (mostly plagioclases) created a secondary porosity and enhanced the primary porosity of Upper Mannville reservoir rocks. According to the quantification made on the two samples 01-19 and 13-27 *(Fig. 14, 15)*, the porosity increased repectively by 16.2% and 13.1%, which are representative values for the studied samples. However, this secondary porosity was partially to completely filled by carbonate cements. This may also explain the negative correlation between proportions of quartz/feldspars and carbonate cements. The more quartz and feldspars dissolved, the more space for the precipitation of carbonate cement exists.

Impact of Carbonate Cements
The invoked mechanism to explain the carbonate authigenesis within the Upper Mannville includes the circulation at depth of meteoric fluids towards the foreland eastward, the recharge area being the exposed part of the chain in the West (topographic-driven flow after Garven and Freeze, 1984), and a recharge area located at the eastern edge of the basin at shallow depth, responsible for "tar sands" biodegradation in

Athabasca (Schneider, 2003). Furthermore, for the carbonate samples showing $\delta^{13}C$ values more negative compared to those reported in literature (Longstaffe and Ayalon, 1987; Connolly *et al*., 1990), it has been proposed a complementary carbon source component, related to the production of organic acides from organic matter maturation. If we accept these interpretations we can draw two hypothesis on the controls operated by the carbonate phase distribution on the reservoir quality.

As the topographic-driven flow and the mixing of meteoric water with formation fluids is the mechanism to explain the fluid-flow towards the foreland basin, more carbonates should be expected in the West and less in the East. A systematic investigation of the proportion of carbonate cement in these reservoir at regional scale would help backing up this hypothesis.

As the carbon which entered the carbonate structures was partially derived from the organic matter maturation, more carbonates should be expected within the organic-rich sediments. The spatial relationship between the horizons richer in organic matter and those more affected by carbonate replacement and cements could also be investigate verify this hypothesis.

The main controls on the reservoir quality directly derive from the initial mineralogy of the reservoir rocks, which depends on the source of sediments (Rocky Mountains), and on the physico-chenical processes involved in the sedimentation. At a regional scale, we can expect more clay-rich sediments in the downstream part of the system, as the fluvial energy decrease, associated with moderate carbonate cementation and a better preserved porosity. However, very high clay content may have adverse effect on reservoir quality. At a reservoir scale, finning upward sequences of the channel infill, also records a decrease of depositional energy. As a consequence, an upward increase of the clay minerals content in the fluvial channel fill sequence is expected.

CONCLUSION

The Upper Mannville incised valley fills have experienced significant burial diagenetic processes that have strongly influenced the reservoir quality.

The initial mineralogical composition directly controls the effects of diagenesis, mostly during mesogenesis and telogenesis. Initial clay mineral content is directly affecting the amount of carbonate cement that precipitated in the Upper Mannville fluvial reservoirs. The best reservoir rocks have a significant clay content that prevented from intense carbonate cementation. The low clay-bearing reservoir rocks are intensively or completely plugged by carbonate cements.

Carbonates precipitated under deep burial conditions, during collisional tectonics by an influx of meteoric fluids driven by a high hydraulic head, compatible with the

presence of an orogen (recharging area) in the West already largely exhumated. The timing of carbonate origin is therefore inferred from the chosen meteoric recharge model, which implies the presence of an already exposed recharge area (*i.e.* the orogen in the West) to permit the meteoric fluids the feed the hydrodynamic system at depth.

Quantification of diagenetic phases and reconstitution of both texture and mineralogy at each important steps of the paragenesis may help quantifying material balance through the reservoir history. This may help predicting diagenetic heterogeneities at both the basin and the reservoir scale.

ACKNOWLEDGMENTS

REFERENCES

Aagaard P., Egeberg P.K., Saigal G.C., Morad S., Bjorlykke K. (1990) Diagenetic albitization of detrital K-feldspars in Jurassic, Lower Cretaceous and Tertiary clastic reservoir rocks from offshore Norway, II: Formation water chemistry and kinetic considerations, *J. Sediment. Petrol.* **60**, 575-581.

Aase N.E., Bjørkum P.A., Nadeau P. (1996) The effect of grain coating microquartz on preservation of reservoir porosity, *AAPG Bull.* **80**, 1654-1673.

Bachu S. (1999) Flow Systems in the Alberta Basin: Patterns, Types and Driving Mechanisms, *Bull. Can. Pet. Geol.* **47**, 4, 455-474.

Berner R.A. (1984) Sedimentary pyrite formation: an update, *Geochim. Cosmochim. Acta* **48**, 605-615.

Blake R.E., Walter L.M. (1999) Kinetics of feldspar and quartz dissolution at 70-80°C and near-neutral pH: effects of organic acids and NaCl, *Geochim. Cosmochim. Acta* **63**, 13-14, 2043-2059.

Bloch S., Helmond K.P. (1995) Approaches to predicting reservoir quality in sandstones, *AAPG Bull.* **79**, 97-115.

Butler I.B., Rickard D. (2000) Framboidal pyrite formation via the oxidation of iron (II) monosulphide by hydrogen sulphide, *Geochim. Cosmochim. Acta* **64**, 2665-2672.

Cant D.J., Stockmal G.S. (1989) The Alberta foreland basin: relationship between stratigraphy and Cordilleran terrane-accretion events, *Can. J. Earth Sci.* **26**, 1964-1975.

Cant D.J. (1996) Sedimentological and sequence stratigraphic organization of a foreland clastic wedge, Mannville Group, Western Canada Basin, *J. Sediment. Res.* **66**, 6, 1137-1147.

Claeys P.F., Mount J.F. (1991) Diagenetic origin of carbonate, sulfide, and oxide inclusions in biotites of the Great Valley Group (Cretaceous), Sacramento Valley, California, *J. Sediment. Petrol.* **61**, 719-731.

Connolly C.A., Walter L.M., Baadsgaard H., Longstaffe F.J. (1990) Origin and evolution of formation waters, Alberta Basin, Western Canada Sedimentary Basin. II. Isotope systematics and water mixing, *Appl. Geochem.* **5**, 397-413.

Creaney S., Allan J., Cole K.S., Fowler M.G., Brooks P.W., Osadetz K.G., Macqueen R.W., Snowdon L.R., Riediger C.L. (1994) Petroleumgeneration and migration in the Western Canadian sedimentary basin, Mossop G., Shetson I. (eds), *Canadian Society of Petroleum Geologists and Alberta Research Council*, Calgary, Alberta, pp. 455-468.

Curtis C.D., Pearson M.J., Somogyi V.A. (1975) Mineralogy, chemistry and origin of a concretionary siderite sheet (clay-ironstone band) in the Westphalian of Yorkshire, *Mineral. Mag.* **40**, 385-93.

De Andrade V., Vidal O., Lewin E., O'Brien P., Aagard P. (2006) Quantification of electron microprobe compositional maps of rocks thin sections: an optimized method and examples, *J. Metamorph. Geol.* **24**, 655-668.

De Ros L.F., Morad S., Paim P.S.G. (1994) The role of detrital composition and climate on the diagenetic evolution of the continental molasses: evidence from Cambro-Ordovician Guaritus sequences, south Brazil, *Sediment. Geol.* **92**, 197-228.

De Ros L.F. (1996) Compositional controls on sandstone diagenesis, Comprehensive Summaries of Uppsala Dissertations from the Faculty of Science and Technology, Vol. 198, pp. 1-24.

Deschamps R., Euzen T., Delamaide E., Feuchtwanger T., Pruden A. (2008) The Upper Mannville Incised Valleys of Central Alberta: An Example of Subtle Gas Traps, extended abstract, *CSPG CSEG CWLS Joint Annual Convention*, Calgary, 12-14 May.

Dimitrakopoulos R., Muehlenbachs K. (1987) Biodegradation of petroleum as a source of 13C-enriched carbon dioxide in the formation of carbonate cement, *Chem. Geol.* **65**, 283-291. (Isotope Geoscience Section).

Ehrenberg S.N. (1991) Kaolinized, potassium-leached zones at the contacts of the Garn Formation, Haltenbanken, mid-Norwegian continental shelf, *Mar. Petrol. Geol.* **8**, 250-269.

Ehrenberg S.N. (1993) Preservation of anomalously high porosity in deeply buried sandstones by grain-coating chlorite: Examples from the Norwegian continental shelf, *AAPG Bull.* **77**, 1260-1286.

Ehrenberg S.N., Boassen T. (1993) Factors controlling permeability variation in sandstones of the Garn Formation in Trestakk Field, Norwegian continental shelf, *J. Sediment. Petrol.* **5**, 929-944.

Eisbacher G.H., Carrigy M.A., Campbell R.B. (1974) Paleodrainage patterns and late-orogenic basins of the Canadian Cordillera in *Tectonics and Sedimentation*, Dickinson W.R. (ed.), *Society of Economic Paleontologists and Mineralogists, Special Publication* **22**, 143-166.

Eslinger E., Pevear D. (1988) Clay Minerals for Petroleum Geologists and Engineers. SEPM Short Course Notes no. 22. ix + 405 pp., *Society of Economic Paleontologists and Mineralogists*, Tulsa.

Euzen T., Power M., Sliwinski J., Lenormand R., Deschamps R., Durand O. (2010) Advanced reservoir characterization: key to unlocking gas resources of the Upper Mannville incised valley systems (Lower Cretaceous, West-central Alberta), Abstract, *CSPG CSEG CWLS Joint Annual Convention*, Calgary, 10-14 May.

Euzen T., Burns S., Power M., Deschamps R., Lenormand R. (2011) Influence of Mineralogy and Macroporosity on Reservoir Quality: Example of the Upper Mannville Incised Valley Fills in West-Central Alberta, Abstract, *CSPG CSEG CWLS Joint Annual Convention*, Calgary, 9-12 May.

Faure J.L., Osadetz K., Benaouli Z.N., Schneider F., Roure F. (2004) Kinematic and Petroleum Modeling of the Alberta Foothills and Adjacent Foreland - West of Calgary, *Oil Gas Sci. Technol. – Rev. IFP* **59**, 1, 81-108.

Folk R.L. (1974) *The petrology of sedimentary rocks*, Hemphill Publishing Co., Austin, Texas, 182 p.

R Deschamps et al. / *Impact of Mineralogy and Diagenesis on Reservoir Quality of the Lower Cretaceous Upper Mannville Formation (Alberta, Canada)*

57

Freed R.L., Peacor D.R. (1989) TEM lattice fringe images with R1 ordering of illite/smectite in Gulf Coast pelitic rocks (abstract), *Geol. Soc. Am.* **21**, A16. Abstracts with Programs.

Friedman I., O'Neil J.R. (1977) Compilation of stable isotope fractionation factors of geochemical interest, in *US Geological Survey Professional*, Paper 440 KK, 12 p.

Garven G., Freeze R.A. (1984) Theoretical analysis of the role of groundwater flow in the genesis of stratabound ore deposits. 2. Quantitative results, *Am. J. Sci.* **284**, 1125-1174.

Gradusov P.P. (1974) A tentative study of clay mineral distribution in soils of the world, *Geoderma* **12**, 1-2, 49-55, Special Issue Soil Science in the U.S.S.R.

Grigsby J.D. (2001) Origin and growth mechanism of authigenic chlorite in sandstones of the Lower Vicksburg Formation, south Texas, *J. Sediment. Res.* **71**, 27-36.

Hallam A. (1985) A review of Mesozoic climates, *J. Geol. Soc London* **142**, 433-445.

Hancock N.J. (1978) Possible causes of Rotliegend sandstone diagenesis in northern West Germany, *J. Geol. Soc. London* **135**, 35-40.

Hancock N.J., Taylor A.M. (1978) Clay mineral diagenesis and oil migration in the Middle Jurassic Brent sand formation, *J. Geol. Soc. London* **135**, 69-72.

Hayes B.J.R., Christopher J.E., Rosenthal L., Loss J., McKercher B. (1994) Cretaceous Mannville Group of Western Canada, in *Geological Atlas of the Western Canada Sedimentary Basin. Canadian Society of Petroleum Geologists and Alberta Research Council*, Mossop G.D., Shetsen I. (eds), pp. 317-334.

Higley K.D., Lewan M.D., Roberts L.N., Henry M. (2009) Timing and petroleum sources for the Lower Cretaceous Mannville Group oil sands of Northern Alberta based on 4-D modelling, *AAPG Bull.* **93**, 2, 203-230.

Hower J., Eslinger E.V., Hower M.E., Perry E.A. (1976) Mechanism of burial metamorphism of argillaceous sediments: 1. Mineralogical and chemical evidence, *Geol. Soc. Am. Bull.* **87**, 725-737.

Irwin H., Curtis C., Coleman M. (1977) Isotopic evidence for source of diagenetic carbonates formed during burial of organic rich sediments, *Nature* **269**, 209-213.

Jackson P.C., Masters J.A., (eds) (1984) Elmworth – Case Study of a Deep Basin Gas Field. Paleogeography of the Lower Cretaceous Mannville Group of Western Canada, *AAPG Memoir* **38**, 49-78.

Karavas F.A., Riediger C.L., Fowler M.G., Snowdon L.R. (1998) Oil families in Mannville Group reservoirs of southwestern Alberta, Western Canada Sedimentary Basin, *Org. Geochem.* **29**, 769-784.

Land L.S. (1983) The application of stable isotopes to studies of the origin of dolomite and to problems of diagenesis of clastic sediments in *Stable Isotopes in Sedimentary Geology*, Arthur M.A., Anderson T.F., Kaplan I.R., Veizer J., Land L.S. (eds), *Society of Sedimentary Geology Short Course* **10**, 4.1-4.22.

Lanson B., Beaufort D., Berger G., Bauer A., Cassagnabere A., Meunier A. (2002) Authigenic kaolin and illitic minerals during burial diagenesis of sandstones: a review, *Clay Miner.* **37**, 1-22.

Longstaffe F.J., Ayalon A. (1987) Oxygen-isotope studies of clastic diagenesis in the Lower Cretaceous Viking Formation, Alberta: implication for the role of meteoric water, in *Diagenesis of sedimentary sequences*, Marshall J.D. (ed.), *Geol. Soc. Spec. Pub.* **36**, 277-296.

Macaulay C.I., Fallick A.E., McLaughlin O.M., Haszeldine R.S., Pearson M.J. (1998) The significance of $\delta^{13}C$ of carbonate cements in reservoir sandstones: a regional perspective from the Jurassic of the northern North Sea, in *Carbonate cementation of sandstones*, S. Morad (ed.), Spec Publ., *Int. Assoc. Sedimentol.* **26**, 395-408, Blackwells, Oxford, UK.

Macaulay C.I., Fallick A.E., Haszeldine R.S., Mcaulay G.E. (2000) Oil migration makes the difference: regional distribution of carbonate cement $\delta^{13}C$ in northern North Sea Tertiary sandstones, *Clay Miner.* **35**, 69-76.

Marcelo J., Ketzer M. (2002) Diagenesis and Sequence Stratigraphy: An Integrated Approach to Constrain Evolutin of Reservoir Quality in Sandstones, Comprehensive Summaries of Uppsala Dissertations from the Faculty of Science and Technology, Vol. 762.

Meunier A., Velde B. (2004) *Illite: origin, evolution and metamorphism*, Springer, Berlin, New York, 286 p.

Meunier A. (2005) *Clays*, Springer, 472 p., ISBN: 3-540-21667-7.

Morad S., Ketzer J.M., De Ros F. (2000) Spatial and temporal distribution of diagenetic alterations in siliciclastic rocks: Implications for mass transfer in sedimentary basins, *Sedimentology* **47**, 95-120.

Morad S., Al-Ramadan K., Ketzer J.M., De Ros L.F. (2010) The impact of diagenesis on the heterogeneity of sandstone reservoirs: A review of the role of depositional facies and sequence stratigraphy, *AAPG Bull.* **94**, 1267-1309, doi:10.1306/04211009178.

Morse J.M., MacKenzie F.T. (1990) *Geochemistry of sedimentary carbonates*, Elsevier, Amsterdam, 707 p.

Norris D.K. (1964) The Lower Cretaceous of the southeastern Canadian Cordillera, *Bull. Can. Pet. Geol.* **12**, 201-237.

Osadetz K.G. (1989) Basin analysis applied to petroleum geology in Western Canada, in *Western Canada Sedimentary Basin: A Case History*, Ricketts B.D. (ed.), *Canadian Society of Petroleum Geologists*, 87-302.

Perry E.A. Jr, Hower J. (1972) Late-stage dehydration in deeply buried pelitic sediments, *AAPG Bull.* **56**, 2013-2021.

Pittman E.D. (1989) *Problems related to clay minerals in reservoir sandstones*, Mason J.F., Dickey P.A. (eds), *Oil field development techniques: Proceedings of the Daqing International Meeting: AAPG Studies in Geology* **28**, 237-244.

Pittman E.D., Larese R.E., Heald M.T. (1992) Clay coats: Occurrence and relevance to preservation of porosity in sandstones, Houseknecht D.W., Pittman E.D. (eds), *Society of Economic Paleontologists and Mineralogists* **47**, 241-255, (Special Publication).

Posamentier H.W., Vail P.R. (1988) Eustatic controls on clastic deposition. II. Sequence and systems tract models, in *Sea-Level Changes – An Integrated Approach*, Wilgus C.K., Hastings B.S., Posamentier H.W., Van Wagoner J., Ross C.A., Kendall C.G.St.C. (eds), *SEPM* **SP042**, 125-154. Special Publication.

Posamentier H.W., Jervey M.T., Vail P.R. (1988) Eustatic controls on clastic deposition. I. Conceptual framework, in *Sea-Level Changes – An Integrated Approach*, Wilgus C.K., Hastings B.S., Posamentier H.W., Van Wagoner J.C., Ross C.A., Kendall C.G.St.C. (eds), *SEPM* **SP042**, 10-124. Special Publication.

Postma D. (1982) Pyrite and siderite formation on brackish and freshwater swamp sediments, *Am. J. Sci.* **282**, 1151-1183.

Putnam P.E. (1982) Aspects of the petroleum geology of the Lloydminster heavy oil fields, Alberta and Saskatchewan, *Bull. Can. Pet. Geol.* **30**, 81-111.

Poulton T.P., Christopher J.E., Hayes B.J.R., Losert J., Tittemore J., Gilchrist R.D. (1994) Jurassic and Lowermost Cretaceous strata of the Western Canada Sedimentary Basin, in *Geological Atlas of the Western Canada Sedimentary Basin*, Mossop G.D., Shetsen I. (eds), *Canadian Society of Petroleum Geologists and Alberta Research Council*, pp. 297-316.

Rateev M.A., Sadchikova T.A., Shabrova V.P. (2008) Clay minerals in recent sediments of the world ocean and their relation to type of lithogenesis, *Lithol. Miner. Resour.* **43**, 125-135.

Riediger C.L., Fowler M.G., Snowdon L.R. (1997) Organic geochemistry of the Lower Cretaceous Ostra- code zone, a brackish/nonmarine source for some lower Mannville oils in southeastern Alberta, *Canadian Society of Petroleum Geology Memoir* **18**, 93-102.

Riediger C.L., Fowler M.G., Snowdon L.R., Mac-Donald R., Sherwin M.D. (1999) Origin and alteration of Lower Cretaceous Mannville Group oils from the Provost oil field, east-central Alberta, Canada, *Bull. Can. Pet. Geol.* **47**, 1, 43-62.

Saigal G.C., Morad S., Bjrlykke K., Egeberg P.K., Aagaard P. (1988) Diagenetic albitization of detrital K-feldspar in Jurassic, Lower Cretaceous and Tertiary c1astic reservoir rocks from offshore Norway. 1. Textures and origin, *J. Sediment. Petrol.* **58**, 6, 3-13.

Schneider F. (2003) Basin Modeling in Complex Area: Examples from Eastern Venezuelan and Canadian foothills, *Oil Gas Sci. Technol. – Revue de l'IFP* **58**, 2, 313-324.

Strobl R.S. (1988) The effects of sea-level fluctuations on prograding shoreline sand estuarine valley-fill sequences in the Glauconitic member, Medicine River field and adjacent areas, in *Sequences, Sedimentology: Surface and Subsurface*, James D.P., Leckie D.A. (eds), *Canadian Society of Petroleum Geologists Memoir* **15**, 221-236.

Van De Kamp P.C., Leake B.E. (1996) Petrology, geochemistry, and Na metasomatism of Triassic-Jurassic non-marine clastic sediments in the Newark, Hartford, and Deerfield rift basins, northeastern USA, *Chem. Geol.* **133**, 89-124.

Veizer J., Ala D., Azmy K., Bruckschen P., Buhl D., Bruhn F., Carden G.A.F., Diener A., Ebneth S., Godderis Y., Jasper T., Korte C., Pawellek F., Podlaha O.G., Strauss H. (1999) $^{87}Sr/^{86}Sr$, $\delta^{13}C$ and $\delta^{18}O$ evolution of Phanerozoic seawater, *Chem. Geol.* **161**, 59-88.

Walker T.R., Waugh B., Crone A.J. (1978) Diagenesis in first cycle desert alluvium of Cenozoic age southwestern United States and northwestern Mexico, *Bull. Geol. Soc. Am.* **89**, 19-32.

Weaver C.E. (1989) *Clays, Muds and Shales*, Elsevier, Amsterdam, 818 pp.

Worden R.H., Burley S.D. (2003) Sandstone diagenesis: the evolution of sand to stone, in *Sandstone Diagenesis: Recent and Ancient*, Burley S.D., Worden R.H. (eds), *International Association of Sedimentologists* **4**, 3-44, Reprint Series.

Worden R., Morad S. (2003) Clay minerals in sandstones: Controls on formation, distribution and evolution, in *Clay cements in sandstones*, Worden R.H., Morad S. (eds), *International Association Sedimentologists* **34**, 3-41, Special Publication.

Wyld S.J., Umhoefer P.J., Wright J.E. (2006) Reconstructing northern Cordilleran terranes along known Cretaceous and Cenozoic strike-slip faults: Implications for the Baja British Columbia hypothesis and other models, in *Paleogeography of the North American Cordillera: Evidence For and Against Large-Scale Displacements*, Haggart J.W., Enkin R.J., Monger J.W.H. (eds), *Geological Association of Canada* **46**, 277-298, Special paper.

Wright G.N. (ed.) (1984) *The Western Canada Sedimentruy Basin, a series of geological sections illustrating basin stratigraphy and structure*, Canadian Society of Petroleum Geologists and the Geological Association of Canada.

Zhang G., Jasi D.P., Dong H. (2004) Bioavailability of organic matter intercalated into nontronite clay. *The Clay Minerals Society 41st Annual Meeting*, Richland, Washington, 19-24 June.

Zodrow E.L., Lyons P.C., Millay M. (1996) Geochemistry of autochthonous and hypautochthonous siderite-dolomite coal balls Foord Seam, Bolsovian, Upper Carboniferous, Nova Scotia, Canada, *Int. J. Coal Geol.* **29**, 199-216.